OVEREXPRESSION OF A RHAMM PROTEIN (EXONS 6-14) REDUCES CONTACT INHIBITION IN 10T½ FIBROBLASTS

By

GENEVIEVE DEIDRE CURPEN

A THESIS

SUBMITTED TO THE FACULTY OF GRADUATE STUDIES

IN PARTIAL FULFILLMENT OF THE REQUIREMENTS

FOR THE DEGREE OF

MASTER OF SCIENCE

DEPARTMENT OF PHYSIOLOGY

INSTITUTE OF CELL BIOLOGY

UNIVERSITY OF MANITOBA

WINNIPEG, MANITOBA

ISBN 0-612-13054-1

Canada

Name Genevieve Deidre Curpen.

Dissertation Abstracts International is arranged by broad, general subject categories. Please select the one subject which most nearly describes the content of your dissertation. Enter the corresponding four-digit code in the spaces provided.

Cell. | 0379 | U·M·I

SUBJECT TERM | SUBJECT CODE

Subject Categories

THE HUMANITIES AND SOCIAL SCIENCES

COMMUNICATIONS AND THE ARTS
- Architecture 0729
- Art History 0377
- Cinema 0900
- Dance 0378
- Fine Arts 0357
- Information Science 0723
- Journalism 0391
- Library Science 0399
- Mass Communications 0708
- Music 0413
- Speech Communication 0459
- Theater 0465

EDUCATION
- General 0515
- Administration 0514
- Adult and Continuing 0516
- Agricultural 0517
- Art 0273
- Bilingual and Multicultural 0282
- Business 0688
- Community College 0275
- Curriculum and Instruction 0727
- Early Childhood 0518
- Elementary 0524
- Finance 0277
- Guidance and Counseling 0519
- Health 0680
- Higher 0745
- History of 0520
- Home Economics 0278
- Industrial 0521
- Language and Literature 0279
- Mathematics 0280
- Music 0522
- Philosophy of 0998
- Physical 0523
- Psychology 0525
- Reading 0535
- Religious 0527
- Sciences 0714
- Secondary 0533
- Social Sciences 0534
- Sociology of 0340
- Special 0529
- Teacher Training 0530
- Technology 0710
- Tests and Measurements 0288
- Vocational 0747

LANGUAGE, LITERATURE AND LINGUISTICS
- Language
  - General 0679
  - Ancient 0289
  - Linguistics 0290
  - Modern 0291
- Literature
  - General 0401
  - Classical 0294
  - Comparative 0295
  - Medieval 0297
  - Modern 0298
  - African 0316
  - American 0591
  - Asian 0305
  - Canadian (English) 0352
  - Canadian (French) 0355
  - English 0593
  - Germanic 0311
  - Latin American 0312
  - Middle Eastern 0315
  - Romance 0313
  - Slavic and East European 0314

PHILOSOPHY, RELIGION AND THEOLOGY
- Philosophy 0422
- Religion
  - General 0318
  - Biblical Studies 0321
  - Clergy 0319
  - History of 0320
  - Philosophy of 0322
- Theology 0469

SOCIAL SCIENCES
- American Studies 0323
- Anthropology
  - Archaeology 0324
  - Cultural 0326
  - Physical 0327
- Business Administration
  - General 0310
  - Accounting 0272
  - Banking 0770
  - Management 0454
  - Marketing 0338
- Canadian Studies 0385
- Economics
  - General 0501
  - Agricultural 0503
  - Commerce-Business 0505
  - Finance 0508
  - History 0509
  - Labor 0510
  - Theory 0511
- Folklore 0358
- Geography 0366
- Gerontology 0351
- History
  - General 0578
  - Ancient 0579
  - Medieval 0581
  - Modern 0582
  - Black 0328
  - African 0331
  - Asia, Australia and Oceania 0332
  - Canadian 0334
  - European 0335
  - Latin American 0336
  - Middle Eastern 0333
  - United States 0337
- History of Science 0585
- Law 0398
- Political Science
  - General 0615
  - International Law and Relations 0616
  - Public Administration 0617
- Recreation 0814
- Social Work 0452
- Sociology
  - General 0626
  - Criminology and Penology 0627
  - Demography 0938
  - Ethnic and Racial Studies 0631
  - Individual and Family Studies 0628
  - Industrial and Labor Relations 0629
  - Public and Social Welfare 0630
  - Social Structure and Development 0700
  - Theory and Methods 0344
- Transportation 0709
- Urban and Regional Planning 0999
- Women's Studies 0453

THE SCIENCES AND ENGINEERING

BIOLOGICAL SCIENCES
- Agriculture
  - General 0473
  - Agronomy 0285
  - Animal Culture and Nutrition 0475
  - Animal Pathology 0476
  - Food Science and Technology 0359
  - Forestry and Wildlife 0478
  - Plant Culture 0479
  - Plant Pathology 0480
  - Plant Physiology 0817
  - Range Management 0777
  - Wood Technology 0746
- Biology
  - General 0306
  - Anatomy 0287
  - Biostatistics 0308
  - Botany 0309
  - Cell 0379
  - Ecology 0329
  - Entomology 0353
  - Genetics 0369
  - Limnology 0793
  - Microbiology 0410
  - Molecular 0307
  - Neuroscience 0317
  - Oceanography 0416
  - Physiology 0433
  - Radiation 0821
  - Veterinary Science 0778
  - Zoology 0472
- Biophysics
  - General 0786
  - Medical 0760

EARTH SCIENCES
- Biogeochemistry 0425
- Geochemistry 0996
- Geodesy 0370
- Geology 0372
- Geophysics 0373
- Hydrology 0388
- Mineralogy 0411
- Paleobotany 0345
- Paleoecology 0426
- Paleontology 0418
- Paleozoology 0985
- Palynology 0427
- Physical Geography 0368
- Physical Oceanography 0415

HEALTH AND ENVIRONMENTAL SCIENCES
- Environmental Sciences 0768
- Health Sciences
  - General 0566
  - Audiology 0300
  - Chemotherapy 0992
  - Dentistry 0567
  - Education 0350
  - Hospital Management 0769
  - Human Development 0758
  - Immunology 0982
  - Medicine and Surgery 0564
  - Mental Health 0347
  - Nursing 0569
  - Nutrition 0570
  - Obstetrics and Gynecology 0380
  - Occupational Health and Therapy 0354
  - Ophthalmology 0381
  - Pathology 0571
  - Pharmacology 0419
  - Pharmacy 0572
  - Physical Therapy 0382
  - Public Health 0573
  - Radiology 0574
  - Recreation 0575
  - Speech Pathology 0460
  - Toxicology 0383
- Home Economics 0386

PHYSICAL SCIENCES
Pure Sciences
- Chemistry
  - General 0485
  - Agricultural 0749
  - Analytical 0486
  - Biochemistry 0487
  - Inorganic 0488
  - Nuclear 0738
  - Organic 0490
  - Pharmaceutical 0491
  - Physical 0494
  - Polymer 0495
  - Radiation 0754
- Mathematics 0405
- Physics
  - General 0605
  - Acoustics 0986
  - Astronomy and Astrophysics 0606
  - Atmospheric Science 0608
  - Atomic 0748
  - Electronics and Electricity 0607
  - Elementary Particles and High Energy 0798
  - Fluid and Plasma 0759
  - Molecular 0609
  - Nuclear 0610
  - Optics 0752
  - Radiation 0756
  - Solid State 0611
- Statistics 0463

Applied Sciences
- Applied Mechanics 0346
- Computer Science 0984
- Engineering
  - General 0537
  - Aerospace 0538
  - Agricultural 0539
  - Automotive 0540
  - Biomedical 0541
  - Chemical 0542
  - Civil 0543
  - Electronics and Electrical 0544
  - Heat and Thermodynamics 0348
  - Hydraulic 0545
  - Industrial 0546
  - Marine 0547
  - Materials Science 0794
  - Mechanical 0548
  - Metallurgy 0743
  - Mining 0551
  - Nuclear 0552
  - Packaging 0549
  - Petroleum 0765
  - Sanitary and Municipal 0554
  - System Science 0790
- Geotechnology 0428
- Operations Research 0796
- Plastics Technology 0795
- Textile Technology 0994

PSYCHOLOGY
- General 0621
- Behavioral 0384
- Clinical 0622
- Developmental 0620
- Experimental 0623
- Industrial 0624
- Personality 0625
- Physiological 0989
- Psychobiology 0349
- Psychometrics 0632
- Social 0451

OVEREXPRESSION OF A RHAMM PROTEIN (EXONS 6-14) REDUCES CONTACT INHIBITION IN 10T½ FIBROBLASTS

BY

GENEVIEVE DEIDRE CURPEN

A Thesis submitted to the Faculty of Graduate Studies of the University of Manitoba in partial fulfillment of the requirements of the degree of

MASTER OF SCIENCE

DEDICATED TO MY MOTHER,

FOR HER UNCONDITIONAL LOVE AND SUPPORT

ACKNOWLEDGEMENTS

Many thanks to Dr. Eva Turley for her advice, insightful discussions, and for introducing me to the intriguing world of "Cell Locomotion". To my committee, Dr. Arnold Greenberg, and Dr. David Litchfield, their time, constructive comments, and insight were greatly appreciated. Thanks also to Dr. Jon Gerrard for serving as a committee member during the initial stages of my project. As well, a special thanks to David Litchfield for agreeing to fill the recent position of "thesis committee member" (in spite of his plethora of duties), and for providing me with knowledge that extends beyond the realm of research (tips on how to avoid air borne water). I would also like to acknowledge MHRC for supporting my research.

To the Turley crew, new members and old, thanks for making the laboratory experience particularly memorable. Special thanks to Laurie Lange for her friendship, endless chats, help, and motivating comments. Thanks to Christine Hall for the discussions, "classic" lab moments, and efforts to make fashion a reality in our lab (tips that can undoubtedly be transcended into the real world). A special thanks to Valerie Cripps for being a key contributor to the lab experience - her unique - yet fine sense of humor, sharp comments and inspirational songs will forever be remembered. Carol Wong must also be acknowledged for her participation in the "lab chorus". Rashmin Savani's help (especially his willingness to share his graphing skills), and insistance

that I tackle the slopes, was greatly appreciated. Thanks to Xiuwei Yang for his computer expertise and cheeriness. Joycelyn Entwistle's responses to my questions (and making me "go the distance" to get them), and amusing remarks were also appreciated. A special thanks to Chao Wang for his excellent technical assistance (photocopiers especially), as well as for resounding my name with a ring that was audible enough to be heard throughout the department. Thanks to Shiwen Zhang for his help and Jingbo for her pleasant presence. Ludger Klewes', helpful nature, and "sing song" telephone messages - a good source of entertainment during thesis writing, must also be recognized.

Thanks are also extended to the other members in the department, whose help and smiles were greatly appreciated. A special thanks to Angela Kemp and Eileen McMillan for their technical assistance. Thanks to Marsha Leitch, Linda Verburg, and Sandra Oh, for their eagerness to lend out supplies, as well as their efforts to maintain the Seinfeld Spirit. Acknowledgements are also extended to Arthur Chan, Bill Taylor, Dr. Mowat, Nancy Stewart, Lenka Jarolim, Asim Ashique, and, Feng Deng. Denis Bosc and Dale Klassen (who must be mentioned together), also deserve some recognition for their efforts to make the fountain trips rather interesting.

To my buddies in the main office, Susan Snushner and Agnes Roberecki, their willingness to help was greatly appreciated, and their friendly chats (not to mention their

"right on" sarcasm) will definitely be missed. As well a special thanks to Donna Chornenki for maintaining a warm, friendly and helpful nature, in spite of the "chilly" library environment.

Thanks are also extended to members of the Physiology department, who answered my questions and helped in any way. Special thanks to Kristine Cowley for her "words of wisdom", and witty comments.

To my friends, especially Nageen Hameed, Kevin Heather, and Kathy Shimizu, their optimism, moral support, sense of humor, and friendship, were of great value in maintaining my sanity during the "Pelican Brief".

Finally, I am forever grateful to my mother, Pauline, and brother, Christopher, for their unconditional assistance, support, encouragement, and patience during the course of this project. Not to mention all the late nights my mother willingly prepared delicious take-out dinners, and my brother provided both delivery and "taxi service".

ABSTRACT

Identifying the molecular mechanisms underlying cell migration and growth is critical to understanding normal physiological processes, as well as such pathological conditions as tumorigenesis. A novel hyaluronan (HA) receptor that has been recently cloned (Hardwick *et al.*, 1992), and is referred to by the acronym RHAMM for Receptor for HA Mediated Motility, has been linked to the transformed state by its importance in the motile behavior of *ras*-transformed cells, malignant human B cells, and human breast cancer cells, as well as its effects on cell contact behavior. Based on evidence for RHAMM's involvement in cell locomotion and cell contact behavior, it was predicted that the overexpression of this protein would elicit a transforming effect on the cells. Therefore, a lipofection technique was used to transfect mammalian 10T½ cells, which show strong contact inhibited behavior, with a truncated RHAMM II cDNA (exons 6-14) (Hardwick *et al.*, 1992) in an expression vector containing the ß-actin promoter and a neomycin construct. Stable transfectants were selected by drug resistance, and clones overexpressing the RHAMM protein were identified by Western analysis and subjected to further analysis. Cells overexpressing the RHAMM protein, resembled virally transformed cells in their loss of contact inhibition, as quantitated with a nuclear overlap ratio, and their ability to form foci in monolayer cultures. However, cells did not form

tumors *in vivo*. As well, contrary to control vector transfected cells and the 10T½ parent line, the transfected cells displayed focal contacts that were smaller and resembled those present in motile cells. These results seem to indicate that RHAMM II is involved in conferring a partially transformed phenotype and is consistent with the hypothesis that it does so by disrupting normal cell substratum contacts.

TABLE OF CONTENTS

LIST OF FIGURES AND TABLES

LIST OF ABBREVIATIONS

DMEM	Dulbecos Modified Eagle's Medium
ECM	Extracellular matrix
EDTA	Ethylene-diaminetetraacetic acid
FAK	Focal Adhesion Kinase
FCS	Fetal calf serum
HA	Hyaluronan
HARC	HA Receptor Complex
kb	Kilobase
kDa	KiloDalton
PAGE	Polyacrylamide gel electrophoresis
PCR	Polymerase chain reaction
PEG	Polyethylene glycol
PKC	Protein Kinase C
RHAMM	Receptor for HA Mediated Motility
RT-PCR	Reverse transcriptase PCR
SDS	Sodium dodecyl sulphate
SH2	Src Homology 2 domains
SH3	Src Homology 3 domains

INTRODUCTION

Cell growth and motility represent two biological phenomena that are critical to tumor progression *in vivo* (Zetter, 1990; Giancotti and Mainiero, 1994). Deregulated growth results in the unrestrained cellular proliferation associated with tumor development, and aberrant locomotion contributes to the invasion and metastatic spread of the tumor (Liotta, 1992; Aznavoorian *et al.*, 1993). *In vitro*, cellular transformation is evident in the cells' loss of contact inhibited behavior of growth and movement. Thus the normal suppression of growth and movement that occur when cells make contact with one another are lost (Abercrombie, 1970; Abercrombie *et al.*, 1970; Abercrombie *et al.*, 1971; Alberts *et al.*, 1989; Bray, 1992). Although the understanding of the mechanisms regulating the transformed phenotype are still in its infancy, it is clear that focal adhesions, extracellular matrix (ECM) components, and their receptors, play critical roles in cell contact inhibited behavior and tumorigenesis (Schreiner *et al.*, 1991; Albelda, 1993; Behrens, 1993; Damsky and Werb, 1992; Hynes, 1992; Jones *et al.*, 1993; Ratner, 1992; Ruoslahti, 1992; Schwartz, 1993; Stetler-Stevenson *et al.*, 1993).

Focal adhesions have long been linked to the contact inhibited behavior prevalent in non-transformed cells (Ruoslahti, 1992; Schwartz, 1993; Giancotti and Mainiero, 1994). Since both transformed and motile cells display less

stable focal adhesions than normal contact inhibited and stationary cells (Burridge *et al.*, 1988; Lo and Chen, 1994), these sites are implicated as likely targets in cellular transformation. Focal adhesions represent specialized junctions in which the integrin family of transmembrane receptors mediate cell signalling events that link the ECM to the cytoskeleton (Burridge *et al.*, 1988; Woods and Couchman, 1988; Lo and Chen, 1994). Indeed, the integrins have been found to be important in maintaining cell contact behavior and suppressing tumorigenic capabilities by mediating cell adhesions and transducing signals that affect the cytoskeletal organizations relevant to cell growth and motility (Giancotti and Mainiero, 1994; Juliano, 1994; Lo and Chen, 1994). The overexpression of the $\alpha_5\beta_1$ integrin receptor partially reverts the transformed chinese hamster ovary (CHO) cells to the contact inhibited state by promoting stable focal adhesions (Giancotti and Ruoslahti, 1990). As well, the overexpression of fibronectin integrin receptors reduces tumorigenicity (Giancotti and Ruoslahti, 1990; Symington, 1990; Varner *et al.*, 1992). Reports also indicate that changes in integrin expression may facilitate tumor cell invasion and metastasis (Boukerche *et al.*, 1989; Plantefaber and Hynes, 1989; Ruoslahti and Giancotti, 1989; Giancotti and Mainiero, 1994). Consistent with this, the overexpression of the $\alpha_4\beta_2$ integrin receptor suppresses invasion during tumor cell metastasis (Qian *et al.*, 1994).

Other ECM molecules and their receptors have been linked to tumorigenesis by their effects on growth and locomotion. Some of these proteins' effects on invasion and metastasis occur in association with alterations in focal adhesions. For instance, the overexpression of the extracellular matrix component, thrombospondin, confers anchorage and serum independent growth (Castle *et al.*, 1993), concomitant with a reduction in focal adhesions (Murphy-Ullrich and Hook, 1989). The ECM protein, tenascin, has also been connected to tumorigenesis through its association with focal adhesion disassembly (Murphy-Ullrich *et al.*, 1991; Borsi *et al.*, 1992). Expression of the high affinity laminin receptor and laminin also correlated with tumor invasiveness (Stetler-Stevenson *et al.*, 1993).

The ECM component, hyaluronan (HA), has also been implicated in tumorigenesis (Turley and Tretiak, 1985; Turley, 1992;; Knudson *et al.*, 1984; Knudson *et al.*, 1989; Knudson and Knudson, 1993; Fraser and Laurent, 1993), by its increased prevalence in tumor associated stroma (Turley *et al.*, 1984; Iozzo, 1985; Knudson *et al.*, 1989), and in the conditioned medium of highly metastatic cell lines (Turley *et al.*, 1991; Fraser and Laurent, 1993; Knudson and Knudson, 1993). Elevated HA expression also corresponds with increased cell locomotion, which is characteristic of tumor cells (Turley *et al.*, 1987; Turley *et al.*, 1991; Knudson *et al.*, 1989). Most notably, HA and its receptors, CD44 and RHAMM (acronym for

Receptor for HA Mediated Motility), have been linked to tumor cell locomotion and invasion (Günthert *et al.*, 1991; Hart *et al.*, 1991; Thomas *et al.*, 1992; Turley *et al.*, 1991, Günthert *et al.*, 1993; Wang *et al.*, submitted). The HA receptor, CD44, has been found to be important in establishing the metastatic phenotype in transformed cells (Günthert *et al.*, 1991; Herrlich *et al.*, 1993), and to be a critical regulator of tumor growth (Sy *et al.*, 1991; Bartolazzi *et al.*, 1994). This last property is due to the HA binding capability of CD44 (Bartolazzi *et al.*, 1994).

A number of studies have implicated RHAMM in tumorigenesis. A role for RHAMM in tumor cell motility was first identified in *ras*-transformed cells (Turley *et al.*, 1991), and more recent evidence has demonstrated it to be a critical regulator of the locomotory capabilities of malignant B lymphocytes (Turley *et al.*, 1993), and human breast cancer cells (Wang *et al.*, submitted). Evidence linking RHAMM to the motile behavior of *ras*-transformed cells included its elevated expression and its concentration in the lamellipodia of migrating cells (Turley *et al.*, 1991; Turley, 1992). As well, its functional significance was demonstrated with antibody blocking studies, in which anti-RHAMM antibodies inhibited the HA promoted locomotion (Turley *et al.*, 1991; Turley, 1992; Turley *et al.*, 1993). Investigations into the molecular basis underlying RHAMM's effects implicate RHAMM activation as initiating a cascade of intracellular signalling events that

regulate focal adhesion turnover (Hall *et al.*, 1994), and ultimately culminate in the cytoskeletal reorganizations relevant to the motile phenotype. In addition to RHAMM's association with tumor cell motility, a further link to the transformed state included an experiment depicting an effect on cell contact behavior (Turley *et al.*, 1985; Turley, 1989). The addition of RHAMM to confluent monolayers allowed the cells to overcome contact inhibited behavior and display increased nuclear overlapping like transformed cells (Turley *et al.*, 1985; Turley, 1989). Based on such evidence for RHAMM's involvement in cell locomotion and contact behavior, it was predicted that the overexpression of the RHAMM protein would elicit a transforming effect on cell behavior.

The genomic RHAMM DNA is comprised of 14 exons interrupted by 13 introns (Entwistle *et al.*, submitted). Alternate splicing results in the identification of three RHAMM isoforms (Figure 1 and 2). The RHAMM cDNAs were isolated from the λgt11 cDNA library. A RHAMM I cDNA encodes exons 1-14, excluding exon 4. A RHAMM IV4 cDNA encodes exons 1-14 inclusively. The RHAMM II cDNA is represented by exons 6-14. These RHAMM isoforms appeared to be targetted to the cytoplasm, cell membrane and extracellular milieu.

Therefore, to begin to assess RHAMM's role in cellular transformation, a RHAMM II cDNA (exons 6-14) (Hardwick *et al.*, 1992) was transfected into nontransformed murine 10T½ fibroblasts that display contact inhibition. Although this

RHAMM cDNA did not encode a strong signal sequence or a hydrophobic domain long enough to span the membrane, its membrane localization was suspected to occur in association with other surface protein(s) RHAMM was originally isolated from the extracellular medium with (Turley, 1984; Turley *et al.*, 1987; Turley, 1992). At that time, the RHAMM receptor was postulated to exist at the surface as part of a complex of proteins (referred to as HARC - acronym for HA Receptor Complex) that included a transmembrane docking protein (Hardwick *et al.*, 1992). Evidence for RHAMM's surface localization include FACS analysis, surface labelling, subcellular fractionation and sensitivity to light protease treatment (Hardwick *et al.*, 1992; Klewes *et al.*, 1993, unpublished data). Although the RHAMM receptor protein was observed to be downregulated from the cell surface as the cells slowed down and became contact inhibited (Turley *et al.*, 1991; Hardwick *et al.*, 1992), the docking protein was believed to be constitutively expressed. This proposal that the cell retains surface binding sites for RHAMM, stemmed from studies in which the purified HA binding protein (RHAMM) showed a saturable high affinity binding to the cell surface of contact inhibited fibroblasts that mimicked the cell's endogenous protein distribution when not contact inhibited (Turley *et al.*, 1985). Therefore, the RHAMM protein generated from the transfections was expected to localize at the cell surface.

The results of this study further implicated RHAMM as a

critical regulator of density dependant contact inhibition, a phenomenon relevant to cell motile behavior and growth. The RHAMM II overexpressing cells' acquisition of an altered phenotype that included loss of contact inhibited behavior was indicative of a partial effect on cellular transformation. Although the mechanism by which RHAMM overexpression modulated cell contact behavior was not defined, the slight reduction in focal contacts suggested that a disruption in the cytoskeleton was likely (Burridge *et al.*, 1988; Hall *et al.*, 1994).

FIGURE 1. Schematic representation of Genomic RHAMM DNA and the RHAMM cDNA isoforms (Entwistle *et al.*, submitted). The entire RHAMM gene is divided into 14 exons (open boxes) interrupted by 13 introns (lines connecting the open boxes). The repeat region (21 amino acids repeated 5 times) occurs in exon 8 and is indicated by a capital R. The HA binding domains designated HA1 and HA2 occur in exon 12 and 13, respectively. The hatched boxes represent the non-coding (nc) regions. The ATG initiation codon and TGA stop codon are indicated. Alternate splicing of the DNA results in three RHAMM isoforms. The three RHAMM cDNAs were obtained from a 3T3 cDNA library in λgt11. (i) The RHAMM I cDNA sequence corresponds with the genomic RHAMM DNA, except for the absence of exon 4. (ii) The RHAMM IV4 cDNA encodes exons 1 to 14 (including exon 4). (iii) The RHAMM II cDNA encodes exons 6-14, and represents the focus for this study.

RHAMM Genomic DNA - (introns and exons)

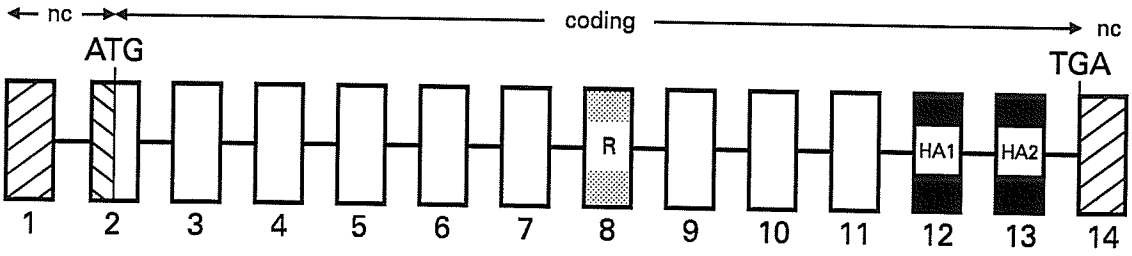

(i) RHAMM I cDNA
(excluding exon 4)

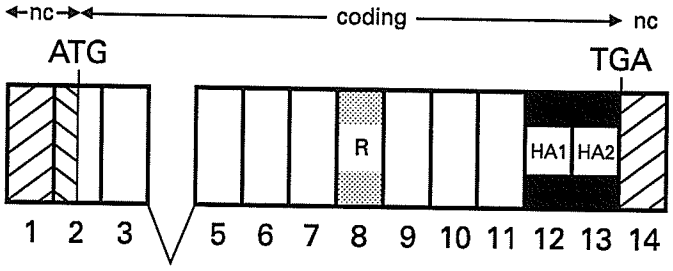

(ii) RHAMM IV4 cDNA
(including exon 4)

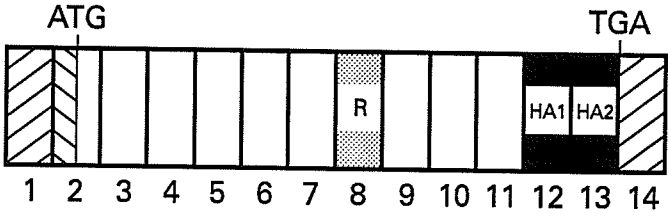

(iii) RHAMM II cDNA

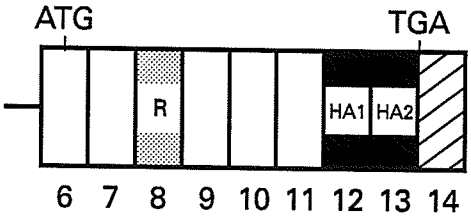

KEY

non-coding

exons

— introns

R Repeat Sequence
(21 amino acids
repeated 5 times)

HA1 HA Binding
Domain I

HA2 HA Binding
Domain 2

FIGURE 2. The nucleotide sequence of the RHAMM exons and flanking sequences. The sequence for all 14 exons and the immediate flanking sequence is indicated. The exon sequences are given in capital letters and the intron sequences in lower case letters. The deduced amino acid sequence is represented by the one letter amino acid code and is placed below the nucleotide sequence and numbered on the left margin (Entwistle *et al.*, submitted). The arrow indicates the start codon for RHAMM II (exons 6-14).

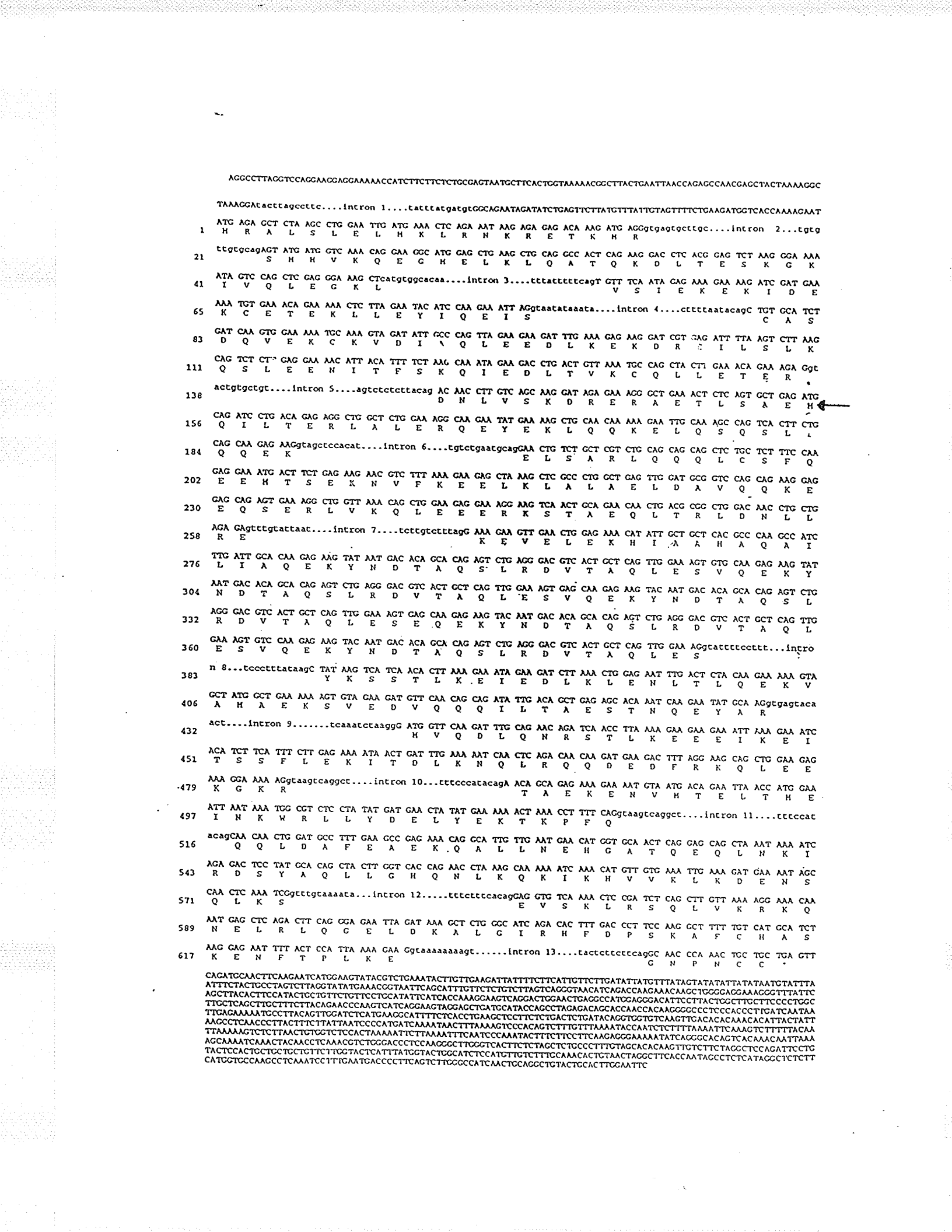

MATERIALS AND METHODS

(1) Cells and Culture

Murine 10T½ fibroblasts were selected as the immortalized cell line to be used in the RHAMM cDNA transfection studies since they exhibited strong contact inhibited behavior in culture (Butler, 1991). Mouse 10T½ fibroblasts were grown in DMEM (Dulbecos Modified Eagle's Medium) (Gibco BRL, Grand Island, NY) containing 10% fetal calf serum (FCS) (Hyclone Laboratories, Ind., Logan, Utah) and 10 mM HEPES, pH 7.4 (Sigma Chemical Co., St. Lousis, MO). The *ras*-transformed C3 (CIRAS) line, derived from 10T½ cells (Egan *et al.*, 1987), the 10T½ RHAMM and control vector transfected clones all harbored a neomycin resistance gene and were therefore cultured at alternate passages in growth medium supplemented with 0.6 mg/ml of geneticin (Gibco). All cell lines were routinely harvested between 80% and 90% confluence using 0.25% trypsin (Difco Bactotrypsin)/2 mM EDTA (Sigma), passaged into 100 mm tissue culture plates (Corning, Corning, NY) at a 1:10 dilution (unless otherwise stated), and maintained at 37°C under 5% CO_2. All cells were used under passage 16. In experiments which required that a specific number of cells be seeded, a viable cell count was determined using trypan blue exclusion (0.4% in PBS) and a hemocytometer (Harlow & Lane; 1988). Frozen stocks of cells were prepared by resuspending the cells in freezing medium (70% DMEM, 20% FCS, and 10% DMSO), and then storing under liquid nitrogen.

(2) Antibodies to RHAMM

The antibody to RHAMM utilized in this study included a rabbit polyclonal (R4) previously shown to block HA (hyaluronan) mediated cell motility (Hardwick *et al.*, 1992; Pilarski *et al.*, 1993; Yang *et al.*, 1993). The antibody (R4) was raised against a synthetic peptide (amino acids 266-288) encoded in the RHAMM cDNA (Hardwick *et al.*, 1992).

The specificity with which the polyclonals interacted with the protein encoded by the RHAMM cDNA was determined by the following criteria (Savani *et al.*, submitted). A) Competition binding to the RHAMM fusion protein using excess fusion protein prevented the anti-peptide antibody from binding to the blotted protein. B) The anti-peptide antibody only recognized bacterially expressed truncated proteins that retained the specific peptide sequence. C) Antiserum that had been depleted of RHAMM antibodies by chromatography on a RHAMM fusion protein affinity column, failed to stain the blotted protein.

(3) Construction of a RHAMM ß-actin Expression Vector

3.1. Purification of the partial RHAMM cDNAs (1.2 kb, 1.7 kb and 1.9 kb) and the Human ß-actin Expression Vector (pHßAPr-1-neo)

The human ß-actin expression vector (pHßApr-1-neo) (Gunning *et al.*, 1987) and the plasmids containing partial RHAMM cDNAs (1.2 kb, 1.7 kb and 1.9 kb) were each purified

from bacteria streaked on L Broth (LB)/ampicillin (100 μg/ml) plates. To purify the plasmid DNA, the host bacteria was initially grown in a 50 ml starter culture inoculated with a single bacterial colony picked from a streaked plate. After incubating the culture overnight in a 37°C shaker, 25 ml of the starter culture was transferred to 500 ml of fresh medium, and the cultures (2x 500 ml) incubated as previously described.

The plasmid DNA was then obtained by alkali lysis of the bacterial cells (Sambrook *et al.*, 1989). Briefly, the cells from each 500 ml culture were pelleted by a 30 minute centrifugation at 3000 rpm, and resuspended in 10 ml of solution I (50 mM glucose -prepared fresh, 25 mM Tris-Cl pH 8.0, and 10 mM EDTA pH 8.0). The two bacterial suspensions (10 ml each) were combined, and the volume was brought up to 40 ml with an additional 20 ml of solution I. 2 ml of a freshly prepared lysozyme solution (10 mg/ml in 10 mM Tris-Cl pH 8.0) was added to lyse the cells, and 80 ml of solution II (0.2 N NaOH freshly diluted from a 10 N stock, and 1% SDS) was added to denature the DNA. The contents were thoroughly mixed, and stored at room temperature for 5 minutes. 40 ml of solution III (58.8 g of potassium acetate dissolved in 30 ml of distilled water, and 170 ml of glacial acetic acid) was then added, the solution mixed and kept on ice for 10 minutes. The bacterial lysate (consisting of chromosomal DNA, high MW RNA and potassium/SDS/protein/membrane complexes) was pelleted

by centrifugation at 6000 rpm for 10 minutes at 4°C. The supernatant was collected, mixed with 0.6 volume of isopropanol, and stored at room temperature for 10 minutes to precipitate the nucleic acids. The nucleic acids were pelleted by centrifugation at 6000 rpm for 15 minutes, rinsed with 70% ethanol and air dried. The pellet was dissolved in 3 ml of TE (0.1 M Tris and 2 mM EDTA pH 8.0), and stored at -20°C until further purification.

The plasmid DNA was then purified by precipitation with polyethylene glycol. The nucleic acid sample was transferred to a 15 ml conical tube containing 6 ml of sterile distilled water. The high molecular weight RNA was precipitated by mixing the sample with 6 ml of 5 M LiCl, and centrifuging at 10,000 rpm for 10 minutes at 4°C. The supernatant was collected and the nucleic acids pelleted by adding an equal volume of isopropanol (12 ml), mixing and centrifuging the sample at 10,000 rpm for 10 minutes at room temperature. The pellet was rinsed with 70% ethanol, air dried, dissolved in 2 ml of TE (pH 8.0) containing DNAase-free pancreatic RNAase (20 μg/ml), and stored at room temperature for 30 minutes. The sample was then mixed with 2 ml of 1.6 N NaCl containing 13% (w/v) polyethylene glycol (PEG 8000), transferred to microfuge tubes, and the plasmid DNA recovered by centrifugation at 12,000 rpm for 5 minutes at 4°C. The supernatants from each microfuge tube were discarded, and 400 μl of TE (pH 8.0) was used to sequentially dissolve each pellet of plasmid DNA. The

solution was then subjected to 3 extractions: once with phenol, once with phenol:chloroform, and once with chloroform. After the final extraction, the aqueous phase (400 μl) was transferred to a fresh microfuge tube, and mixed with 100 μl of 8 M ammonium acetate. Two volumes of absolute ethanol (100%) were added, and the sample stored at room temperature for 10 minutes. The precipitated plasmid DNA was recovered by centrifugation at 12,000 rpm for 5 minutes at 4°C. The supernatant was removed, and 200 μl of 70% ethanol (4°C) was added. The sample was then vortexed briefly, and centrifuged at 12,000 rpm for 2 minutes at 4°C. The supernatant was discarded, and the last traces of ethanol were evaporated. The pellet was dissolved in 500 μl of TE (pH 8.0), and the concentration of plasmid DNA was determined by the $O.D._{260}$ of a 1:100 dilution of the sample (1 OD_{260} = 50 μg of plasmid DNA/ml). The DNA was stored in aliquots at -20°C.

To confirm the identity of the purified plasmid DNA, samples were subjected to a series of restriction digests (based on the sequence), and the fragments size determined by gel electrophoresis.

3.2. Full length RHAMM II cDNA (exons 6-14) generated through ligations

A cDNA, encoding the open reading frame (ORF) for the 55 kDa isoform of RHAMM (Hardwick *et al.*, 1992), was obtained by ligating restriction fragments of the partial RHAMM cDNAs (1.7

kb and 1.9 kb), which had been previously isolated from a λgt11 mouse 3T3 cDNA library (Hardwick *et al.*, 1992). The basis for using the 1.7 kb and 1.9 kb cDNAs in constructing the RHAMM ORF was due to sequence data indicating that each insert contained a single Bgl II restriction site, that was specifically located in the region where the cDNAs overlapped. Therefore a Bgl II digest would create the sticky ends for the cDNA fragments to anneal into a full length RHAMM cDNA.

The restriction fragments, to be used in the ligations, were obtained by doubly digesting the recombinant RHAMM plasmids: the plasmid containing the 1.7 kb cDNA was digested with Sac I and Bgl II; and the plasmid containing the 1.9 kb cDNA was digested with Eco RI and Bgl II. The digested products were electrophoresed on 1% agarose gels and the cDNA fragments purified using Gene Clean (Prep-A-Gene-Kit). The restriction fragments of 1.1 kb (derived from the 1.7 kb cDNA) and 1.5 kb (derived from the 1.9 kb cDNA) were resuspended in 100 μl of TE buffer and stored at -20°C.

Since the full length RHAMM cDNA was to be cloned into the Bluescript plasmid (Stratagene, La Jolla CA), the vector was digested with Eco RI and Sac I in order to create the complementary ends for the RHAMM cDNA insertion. The digest was electrophoresed on agarose (1%) gels and the opened plasmid purified using Prep-A-Gene. After the DNA was resuspended in 50 μl of TE buffer, the sample was stored at -20°C. The two cDNA inserts were then ligated together and

inserted into Bluescript (Yang *et al.*, 1993), using bacteriophage T4 DNA ligase. The ligation of the two cDNAs and their insertion into Bluescript was set up using 0.5 μg of the 1.1 kb cDNA, 1.5 kb cDNA, and the Bluescript plasmid. The ligation mixture was initially incubated at 6°C overnight (since the 15°C control was not functioning), and then at room temperature for 2 hours with an additional μl of ligase.

3.3. Transformation of bacteria with recombinant RHAMM Bluescript

The ligation mixture was transformed into competent XL1-Blue cells. To prepare the competent cells, 100 μl of an overnight culture of XL1-Blue was added to 5 ml of L Broth (LB) (10 g/L Trypton, 5 g/L Yeast Extract, 5 g/L NaCl, pH 7.5), supplemented with $MgCl_2$ (100 μg/ml) to facilitate plasmid adsorption to the bacteria. The culture was incubated in a 37°C shaker for 2.5 hours and then chilled on ice for 20 minutes. The bacterial cells were pelleted by centrifugation at 10,000 rpm for 5 minutes at 4°C, resuspended in 2 ml of ice cold $CaCl_2$ (50 mM) and then kept on ice for 20 minutes. The cells were further concentrated by another centrifugation at 10,000 rpm for 5 minutes at 4°C, and resuspension in 200 μl of $CaCl_2$ (50 mM). The competent cells were then left on ice for a minimum of 20 minutes or until transformation.

For bacterial transformation, the ligation mixture was combined with the competent XL1-Blue cells in a 1:10 volume

ratio, and set on ice for 15 minutes. The cells were heat shocked at 42°C for 2 minutes in order to promote bacterial uptake of the DNA. The sample was then incubated at room temperature for 10 minutes. A ml of prewarmed LB (containing 100 μg/ml of $MgCl_2$) was added, and the mixture was incubated at 37°C without shaking for 45 minutes. The transformation sample was then divided into 500 μl, 200 μl, 50 μl, 20 μl, and 5 μl aliquots. 6 μl of 100 mM IPTG (isopropylthio-B-D-galactoside, a gratuitous inducer of B-galactosidase) and 8 μl (50 mg/ml) of X-gal (5-bromo-4-chloro-3-indolyl-B-D-galactoside, a chromogenic substrate) was added to each aliquot, and a glass rod was used to spread the samples onto 5 LB agar (1.5%) plates containing ampicillin (100 μg/ml) to select cells transformed with the recombinant plasmid. The plates were incubated overnight at 37°C, and then set on ice for 3 hours.

Bacterial colonies transformed with the recombinant RHAMM plasmid, were identified by antibiotic (ampicillin) resistance and colony color in the presence of IPTG and X-gal. Colonies positive for recombinant RHAMM plasmids appeared white, while colonies of negative recombinants were blue. The ampicillin resistant whitish colonies were randomly picked. The bacteria containing the recombinant plasmid was then subjected to a second selection by streaking each colony onto 2 LB/amp plates, and adding 2 μl of IPTG and 2 μl of X-gal to each streak. The plates were incubated overnight at 37°C and then

set at 4°C for 3 hours. After this final selection, 3 white colonies were picked for purification of the recombinant DNA.

3.4. Small scale DNA preparation of the recombinant Bluescript

A small scale preparation of the recombinant RHAMM plasmid (Bluescript containing the full length RHAMM cDNA) was conducted by alkali lysis of the bacteria. For each preparation (3), the selected colony was grown overnight in 10 ml of LB/ampicillin medium in a 37°C shaker. The cells were collected by centrifugation at 4000 rpm for 10 minutes, and resuspended in 5 ml of ice cold STE (0.1 M NaCl, 10 mM Tris-Cl (pH 8.0), 1 mM EDTA (pH 8.0)). The cells were centrifuged again and the pellet resuspended in 1 ml of solution I (50 mM glucose, 25 mM Tris-Cl (pH 8.0), 10 mM EDTA (pH 8.0)). 100 μl of freshly prepared lysozyme (10 mg/ml in 10 mM Tris-Cl, pH 8.0) was added to lyse the cell wall, and 2 ml of solution II (0.2 N NaOH freshly diluted from a 10 N stock and 1% SDS) to promote DNA denaturation. The solution was gently mixed and the reaction was allowed to proceed at room temperature for 10 minutes. The cells were then treated with 1.5 ml of ice cold solution III (60 ml of 5 M potassium acetate, 11.5 ml of glacial acetic acid, and 28.5 ml of distilled water), thoroughly mixed and kept on ice for 10 minutes in order to neutralize the NaOH from the previous step, precipitate the SDS/lipid/protein, and allow the plasmid DNA to completely

renature. The precipitate was pelleted by centrifugation at 5000 rpm for 10 minutes at 4°C, and discarded. The supernatant was collected, mixed with a 0.6 volume of isopropanol and left at room temperature for 10 minutes to precipitate the plasmid DNA. The plasmid DNA was then pelleted by centrifugation at 5000 rpm for 15 minutes at room temperature (since salt may precipitate at lower temperatures). The supernatant was decanted, and the pellet was washed with 75% ethanol, and then dried at room temperature. The sample was resuspended in 350 μl of STE, digested with RNase A (150 μg/ml) for 2 hours at 37°C, and then digested with proteinase K (50 μg/ml) in 0.5% SDS for another 2 hours at 37°C. The DNA was extracted twice with an equal volume of phenol:chloroform and once with an equal volume of chloroform. The DNA was then precipitated with 0.1 volume of 3 M sodium acetate and 2.5 volumes of ethanol. After the precipitate was pelleted by centrifugation at 13,000 rpm for 20 minutes, the DNA pellet was washed with 75% ethanol and then resuspended in 100 μl of TE buffer. To ensure that the cDNA ligation and insertion into the plasmid occurred in the sense orientation, an aliquot of the purified DNA was cut with the restriction enzymes used in constructing the recombinant plasmid. Therefore, the DNA preps were doubly digested for 2 hours at 37°C with two pairs of enzymes: (1) Bgl II and Eco RI (2) Bgl II and Sac I. Single digests with Eco RI, Bgl II and Sac I were also set up under the same conditions. The DNA

used to construct the recombinant vector (purified cDNA restriction fragments of 1.1 kb and 1.5 kb, and the opened Bluescript plasmid) served as controls and were electrophoresed (1% agarose gels) alongside the digested samples. The comparative analysis was used to confirm that the recombinant plasmid comprised the specific restriction fragments.

3.5. Large scale amplification of recombinant Bluescript

The recombinant plasmid DNA of the above three transformed bacterial colonies were amplified in large scale based on protocols outlined by Sambrook *et al.* (1989). For each prep, a single bacterial colony was grown overnight in 1 liter of LB/amp media in a 37°C shaker. In the morning, 5 ml of chloroamphenicol (34 mg/ml) was added to increase the yield of recombinant plasmid DNA, and the culture was incubated for an additional 4 hours at 37°C. The cells were collected by centrifugation at 8000 rpm for 8 minutes and resuspension in 500 ml of ice-cold STE, followed by another centrifugation and resuspension in 100 ml of solution I (recipes of solutions described in Small scale DNA preparation of recombinant Bluescript). 80 mg of freshly prepared lysozyme was then added to lyse the cells, and 200 ml of freshly prepared solution II was added to promote DNA denaturation. The solution was mixed and left at room temperature for 10 minutes. The cells were then treated with 150 ml of ice cold

solution III, thoroughly mixed and kept on ice for 10 minutes. The SDS/lipid/protein precipitate was pelleted by centrifugation at 8000 rpm for 8 minutes at 4°C, and discarded. The supernatant was collected, mixed with 0.6 volume of isopropanol, and kept at room temperature for 10 minutes to precipitate the plasmid DNA. The precipitate was pelleted by a 15 minute centrifugation at 8000 rpm, and resuspended in 80 ml of triton buffer (50 mM Tris-HCl pH 8.0, 50 mM Na_2EDTA, and 0.4% Triton X-100).

The plasmid DNA was then purified on a CsCl-ethidium bromide gradient. The gradient was prepared by combining 80 ml of the DNA solution (in triton buffer) with 80 g of CsCl (8 g of CsCl per 10 ml of DNA) and 0.2 ml of ethidium bromide. The gradients were ultracentrifuged at 60,000 rpm for 20 hours at 10°C and the plasmid DNA (lower band) was collected using a 21-gauge needle as described by Sambrook *et al.* (1989). The CsCl was removed from the DNA solution by subjecting the sample to two, 24 hour dialysis against TE buffer (4 liters, pH 8.0). The dialyzed DNA was then collected in 4 eppendorf tubes (about 5 ml). To confirm that the purified plasmid contained the correct cDNA insert, samples were digested and analyzed as described above.

3.6. PCR Amplification of the RHAMM cDNA Open Reading Frame

The RHAMM cDNA reading frame (1.4 kb) was amplified with polymerase chain reaction (PCR) (Sambrook *et al.*, 1989), using 2 oligonucleotides as primers: one complementary to the translation initiation regions (nucleotide 1-22) creating a Sal I site linked to nucleotide 1; the other complementary to the region 280 bases after the translation stop codon (nucleotide 1685-1706) creating a Hind III site linked to nucleotide 1706 (Yang *et al.*, 1993). Two different preparations of the full length RHAMM cDNA inserted into Bluescript were used as templates in the PCR reaction. The complete 2.9 kb RHAMM cDNA, purified from the λgt11 stock, was used as a control template for the PCR reaction. The PCR reaction was carried out at 94°C (30 sec.), 54°C (30 sec.), 72°C (90 sec.) for a total of 25 cycles (Sambrook *et al.*, 1989). The 3 PCR products were digested with proteinase K (50 μg/ml) in 0.5% SDS at 37°C for 1 hour. The DNA was then extracted from the mixture with an equal volume of phenol/chloroform (1:1), an equal volume of chloroform, and ethanol precipitated (Sambrook *et al.*, 1989). The PCR products (100 μl) were doubly digested with Sal I and Hind III at 37°C overnight. The resulting 1.7 kb cDNAs were purified by agarose (1%) gel electrophoresis, electroelution in a dialysis tube, alcohol precipitation and resuspension in TE.

3.7. Ligation of the RHAMM Open Reading Frame (generated by PCR) into the Human ß-actin Expression Vector

The RHAMM ORF (exons 6-14) was constructed into a mammalian expression vector designated pHßApr1-neo (Figure 3) (Gunning *et al.*, 1987). The vector contains a human ß-actin promoter, consisting of 3 kb of the ß-actin gene 5' flanking sequence, plus a 5' untranslated region (UTR), and an intervening sequence 1(IVS1). This sequence was linked at the 3' splice site to a short DNA polylinker sequence consisting of unique Sal I, Hind III, and Bam HI restriction sites, which was followed by a SV40 polyadenylation signal. The vector also contained a neomycin resistance gene for selection (Gunning *et al.*, 1987). To ligate the full length RHAMM cDNA into the vector, the vector was digested with Hind III and Sal I for 5 hours at 37°C. The digest was then electrophoresed on agarose (1.2%) gels, and the DNA of the cut vector purified by electroeluting the gel fragment in a dialysis tube. The DNA was precipitated with alcohol, and the pellet dried at room temperature, and resuspended in 50 μl of TE buffer (pH 8.0).

The Sal I-Hind III RHAMM cDNA fragment was then ligated into the Sal I and Hind III sites of the pHßApr1-neo plasmid, using 15 ng of the 1.7 kb RHAMM cDNA (PCR product) and 200 ng of the opened ß-actin vector. The ligation was carried out overnight at 15°C with T4 DNA ligase, and then for 2 hours at room temperature with an additional μl of ligase.

FIGURE 3. Schematic of expression vector used in the RHAMM cDNA transfection studies. A RHAMM II cDNA (exons 6-14) insert, encoding the open reading frame, was constructed into an expression vector containing a ß-actin promoter and a selectable neomycin resistance gene.

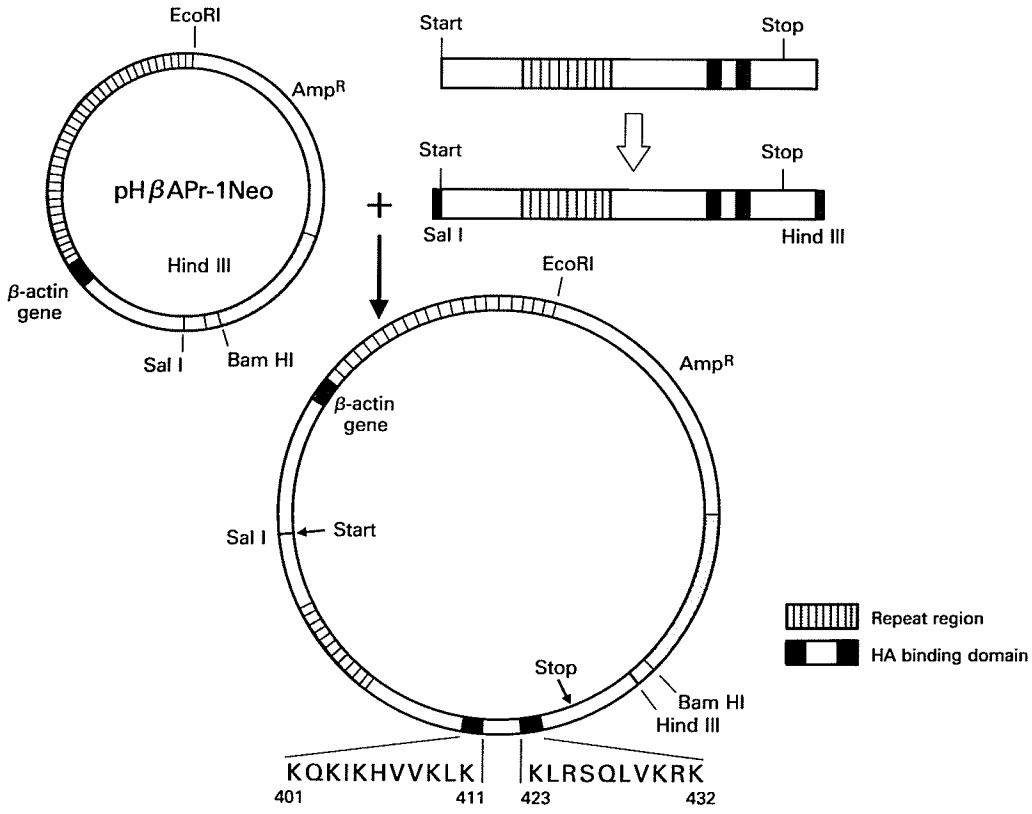
EcoRI
Amp^R
pHβAPr-1Neo
Hind III
β-actin gene
Sal I
Bam HI
Start
Stop
Start
Stop
Sal I
Hind III
EcoRI
Amp^R
β-actin gene
Sal I
Start
Stop
Bam HI
Hind III
KQKIKHVVKLK
KLRSQLVKRK
401
411
423
432
Repeat region
HA binding domain

3.8. Transformation of bacteria with recombinant RHAMM expression vector

The ligation mixture was then transformed into competent *Escherichia coli* HB101 cells as previously described (in the Transformation of bacteria with recombinant Bluescript). However, when concentrating the cells, the bacterial pellet was first resuspended in 3 ml of $CaCl_2$ and then in 0.5 ml.

To transform the bacteria with the recombinant expression vector, the ligation mixture was combined with the competent HB101 cells in a 1:10 volume ratio, along with 50 μl of TFB buffer (10 mM MES, (pH 6.3), 45 mM $MnCl_2.4H_2O$, 10 mM $CaCl_2.2H_2O$, 100 mM KCl, 3 mM Hexamminecobalt chloride; Sambrook *et al.*, 1989). The mixture was set on ice for 15 minutes, then subjected to heat shock at 42°C for 90 seconds, followed by a 10 minute incubation at room temperature. One ml of prewarmed LB/$MgCl_2$ was added, and the transformation mixture was incubated at 37°C for 45 minutes without shaking. A glass rod was used to spread the mixture onto 2 LB/amp plates, which were then incubated overnight at 37°C. The colonies, isolated after bacterial transformation with each of the recombinant DNA preps (3), were streaked onto a master LB/amp agar plate and then grown at 37°C overnight.

3.9. Colony hybridization/ Replica plating

The master plate was chilled at 4°C for 4 hours in order to prevent the agarose from adhering to the membrane filters

in the following step. The bacterial colonies were then replica plated onto a Nylon Hybond N^+ membrane by laying a membrane over the colonies for 1-2 minutes. The membrane was removed, and its orientation with respect to the plate (as described by Sambrook *et al.*, 1989) was noted so the position of the positive recombinants could later be identified. The filters were then sequentially immersed, for 5 minutes each, in denaturing solution (0.5 N NaOH, 1.5 M NaCl), neutralizing solution (1.5 M NaCl, 0.5 M Tris-Cl pH 7.4), and wash solution (2xSCC). The filters were then placed on 3MM paper and left to dry at room temperature (at least 30 minutes). The DNA was fixed to the dried filters by baking for 1-2 hours at 80°C in a vacuum oven (Sambrook *et al.*, 1989). The Hybond N^+ membrane was then screened with a ^{32}P-labelled 1.7 kb partial RHAMM cDNA. To prepare the probe, the cDNA was first separated from the plasmid with a Sac I digest, then purified by agarose gel electrophoresis and gene clean, and labelled according to methods outlined in the Pharmacia Oligolabelling Kit. Prior to the hybridization, the cDNA probe was denatured by heating for 5 minutes at 100°C, and then rapidly chilled on ice. For the screening process, the dried filter was placed into a plastic bag containing prehybridization solution (6X SSC, 5X Denhardt's solution, 0.5% SDS and 20 μg of denatured salmon sperm DNA per ml hybridization solution), the bag sealed and incubated for 4 hours at 65°C. The liquid was then replaced with hybridization solution (prehybridization solution

containing single stranded radiolabelled probe), and the membrane was hybridized overnight at 65°C (as described by Sambrook *et al.*, 1989). After the hybridization, the membrane was sequentially washed at 65°C, for 30 minutes each, with 2xSSC, 1xSSC, and 0.1xSSC. The membrane was exposed to Kodak X-Omat film for 16 hours at -70°C (as Sambrook *et al.*, 1989), and a positive hybridization signal identified the bacterial colonies carrying the recombinant RHAMM expression vector. RHAMM positive colonies were selected by aligning the film with the membrane filter and the master plate (as Sambrook *et al.*, 1989). The plasmid DNA from 4 positive colonies were purified (as described in Small scale DNA preparation of recombinant Bluescript), and analyzed with Sal I and Hind III restriction digests (endonuclease sites defining the ends of the complete RHAMM cDNA), in order to confirm that the plasmid contained the full length RHAMM cDNA.

3.10. Large scale amplification of recombinant RHAMM expression vector

The plasmid DNA, from one of the colonies positive for recombinant RHAMM, was purified in large scale as previously outlined (Large scale amplification of recombinant Bluescript). To confirm that the purified DNA contained the correct cDNA insert, samples were digested with Hind III and Sal I (single and double digests), and the digested products electrophoresed on 0.8% agarose gels.

(4) Transfection by Lipofection

A lipofectin technique (Gibco, BRL) (Felgner, 1987) was used to stably transfect murine 10T½ fibroblasts with the RHAMM II cDNA (exons 6-14) (Entwistle *et al.*, submitted) in a pHß-Apr-1-neo expression vector (Gunning *et al.*, 1987). To ensure that the vector itself did not invoke significant cellular changes, control cells were transfected with the empty vector. The cultures used in the transfections were prepared by seeding 10^5 cells on 60 mm tissue culture plates, and incubating the plates at 37°C in 5% CO_2, until the cells had reached approximately 50% confluency (48 hours), as recommended for stable transfections (Felgner, 1987; Gibco).

For each transfection (per 60 mm dish), 15 µg of the appropriate DNA was diluted to 50 µl in sterile distilled water, and 30 µg of Lipofectin Reagent (stock - 1 mg/ml) was also diluted to 50 µl in sterile distilled water. The DNA and Lipofectin Reagent were diluted in separate polystyrene snap cap tubes in order to avoid precipitation, and the small sample volumes were kept on ice to minimize loss through evaporation.

A 100 µl solution of the lipid-DNA complex was obtained for each dish (transfection), by adding 50 µl of the diluted Lipofectin Reagent to 50 µl of the diluted DNA. The solution was gently mixed by pipetting (vortexing was not recommended), and then incubated for 15 minutes at room temperature to form the lipid-DNA complex (Felgner, 1987). Since the lipid-DNA

complex tends to adhere to polypropylene tubes, polystyrene tubes were used in the procedure (Felgner, 1987).

While the lipid-DNA mixture was incubating, the 10T½ cells were washed twice with 3 ml of serum free Dulbecco's modified Eagle's medium (DMEM), in order to eliminate any remnants of serum which could inhibit the transfection process (Gibco). 3 ml of DMEM was then added to each of the 60 mm tissue culture plates.

After the 15 minute incubation, the 100 μl solution was uniformly added to the cells (60 mm plate) in a dropwise manner (using sterile pipette tips). The plate was gently swirled and the cells incubated at 37°C under 5% CO_2 for 24 hours to allow cellular uptake of the foreign DNA. Each plate of cells was then placed under drug selection by adding 4 ml of growth medium (DMEM containing 20% FCS and 20 mM Hepes, pH 7.4), supplemented with 0.6 mg/ml of geneticin (G418), and incubating the plates as previously. The selective growth medium was replenished every 3 days until the drug resistant cell colonies could be isolated with a micropipet (containing 1 μl of 0.25% trypsin/2 mM EDTA), and expanded as cell lines.

(5) Expression Analysis

5.1. PCR amplification of the RHAMM II cDNA in transfected cells

To confirm that the RHAMM transfectants contained the transfected cDNA, total cellular DNA (of transfectants and

control vector cells) was purified (according to methods described by Sambrook *et al.*, 1989), and used as templates for PCR amplification of the RHAMM open reading frame (ORF). The PCR reaction was performed using primers complementary to the translation initiation codon (nucleotide 1-22) and the region 280 bases after the translation stop codon (nucleotide 1685-1706). The reaction was carried out at 94°C (45 seconds), 56°C (45 seconds), and 72°C (1.5 minutes), for a total of 35 cycles. The PCR reaction mixtures were treated with proteinase K (50 μg/ml) in 0.5% SDS at 37°C for 1 hour. The DNA was then extracted from the mixture with an equal volume of phenol/chloroform (1:1), an equal volume of chloroform, and ethanol precipitated (Sambrook *et al.*, 1989). The PCR products (100 μl) were doubly digested with Sal I and Hind III at 37°C overnight. The DNA of the PCR products were electrophoresed on an agarose (1%) gel, blotted onto a nylon (Hybond N^+) membrane and hybridized with an oligolabelled 1.7 kb partial RHAMM cDNA (as described by Sambrook *et al.*, 1989).

5.2. RT-PCR analysis of the RHAMM II cDNA messsage in transfected cells

Reverse-transcriptase-PCR was used to determine the presence of RHAMM cDNA sense transcripts and was carried out using MMLV reverse transcriptase and the 1st strand cDNA synthesis kit (Clontech, Clontech Lab, Inc., CA). Briefly, total RNA was isolated from parental 10T½, control vector and

RHAMM cDNA transfected cell lines using the guanidinium method (Kingston *et al.*, 1993). RHAMM cDNA was synthesized on 1 μg total RNA template by using oligo dT. An aliquot of the synthesized cDNA was used as the template for subsequent PCR amplification. A sense 5' primer ATG CAG ATC CTG ACA GAG AGG (1-21) and an antisense primer TTG TAG AGT CAA ATT CTC CAG (763-742) were used. The PCR reaction was performed at 94°C (45 sec), 56°C (45 sec) and 72°C (2 min) for 30 cycles. The PCR products were electrophoresed on 1.0% agarose gels and stained with ethidium bromide. Sense fragments were confirmed by Southern blot analysis using a RHAMM cDNA as the probe (Hardwick *et al.*, 1992).

5.3. Cell lysates

Lysates were prepared from cell lines grown to confluence in 100 mm tissue culture plates. To prepare the lysates, the culture media was removed and the cells rinsed twice with cold PBS (2.7 mM KCL, 1.1 mM KH_2PO_4, 138 mM NaCl, and 8.1 mM Na_2HPO_4, at pH 7.2-7.4). The cells were lysed with 0.6 ml of ice cold RIPA Buffer (25 mM Tris, pH 7.2, 0.1% SDS, 1% Triton X-100, 1% sodium deoxycholate, 0.15 M NaCl, 1 mM EDTA) containing a cocktail of protease inhibitors (Sigma chemicals - 1 μg/ml leupeptin, 1000 KU/ml Aprotinin, 1 mM phenylmethylsulfonyl fluoride). The lysates were scraped into microcentrifuge tubes, incubated for 10 minutes on ice and centrifuged at 13,000 rpm for 15 minutes at 4°C. The

supernatants were then collected and aliquoted into microeppendorf tubes for storage at -80°C. The protein concentration of the lysate was determined using the DC protein assay (Biorad Laboratories, Rockville Center, NY) with bovine serum albumin (BSA) standards.

5.4. Western analysis of cell lysates and supernatant media

Western analysis was conducted on cell lysates prepared at confluency, as well as on extracellular media samples. To examine protein expression in the cell lysates, 10 μg of total protein (determined using the DC Bio-Rad protein assay with BSA as a standard) was electrophoresed on SDS polyacrylamide gels (PAGE) (consisting of a 4% stacking gel, and a 10% separating gel; Laemmli, 1970). For the media fractions, in order to determine the amount of RHAMM protein secreted by a unit of cells, the quantity of protein loaded onto the SDS-PAGE gels (as above) was normalized for the number of cells, based on the total protein concentration of the corresponding cell lysate. In this analysis, the maximum amount of protein separated was 15 μg.

Equivalent sample volumes (using RIPA Buffer) were used in order to help prevent the uneven lateral diffusion of protein bands during electrophoresis. The samples were diluted with sample buffer (Laemmli, 1970), heated for 4 minutes at 95°C, cooled on ice, and loaded onto the gel. The prestained molecular weight protein standards (Sigma) were

also heated as above, and 10 μl was applied to the 16 cm gels (LKB-2001 Vertical Electrophoresis System) and 5 μl to the mini-gels (Bio-rad).

Proteins derived from confluent cell lysates and extracellular samples were fractionated on mini-gels and 16 cm thin (0.75 mm) gels. The proteins were separated on the mini-gels at 200 V, and then transferred (Bio-rad) at 4°C for one hour at 100 V, or overnight at 100 mAmps. For the 16 cm gels, proteins were electrophoresed through the stacking gel at 30 mAmps, and through the separating gel at 40 mAmps, and then transblotted (100 mAmps) overnight (16 hours) at 4°C.

After the proteins were fractionated on the gels and electrophoretically transferred to nitrocellulose membranes (as previously described), the membranes were soaked in TBS (50 mM Tris-HCl, pH 7.4, 200 mM NaCl) for 5 minutes at room temperature. The additional protein binding sites were blocked overnight at 4°C with 5% defatted milk in TTBS, and the membranes washed three times (5 minutes each) with TTBS (0.1% Tween-20 in TBS). The membranes were then incubated for 2 hours at room temperature on a rotator (Nutator; Becton, Dickinson and Company, Parsippany, NJ) with 1% defatted milk/TTBS containing an anti-RHAMM polyclonal (1:1000 dilution, R4). To remove excess antibody the membranes were washed 4 times (10 minutes each) with TTBS. The blots probed with the antibodies were then incubated for 1 hour at room temperature with 1% defatted milk/TTBS containing peroxidase-

conjugated goat anti-rabbit (GAR) secondary antibody (1:5000 dilution, Sigma). After the incubation, the blots were washed 5 times (10 minutes each) with TTBS, once with TBS (15 minutes), and then developed using the ECL Western blotting detection system (Amersham International plc, Amersham, UK) according to the manufacturer's instructions. The proteins were detected by exposing the blots to film (Kodak X-Omat XAR-5 film) for various time intervals.

Following the immunodetection, the wet membranes were sealed in plastic bags and stored at 4°C. If the blot was to be reprobed with another antibody, the bound primary and secondary antibodies were removed by submerging the membranes in stripping buffer (100 mM 2-mercaptoethanol, 2% sodium dodecyl sulphate, 62.5 mM tris-HCl pH 6.7) (Amersham) for 30 minutes at 50°C, with periodic agitation. After the membranes were washed twice (10 minutes each) with TTBS at room temperature, the blocking and immunoblotting procedures were performed as described above.

The protein levels were quantified using a densitometer (Model 620 Video densitometer with 1-D Analyst II software, BioRad, Richmond, CA) which approximates the protein amount according to the area of the optical density.

5.5. Assessment of soluble RHAMM

Cells were grown to confluence in 100 mm tissue culture plates (same cultures the cell lysates were prepared from), and the media (about 10 ml) was collected in 15 ml conical tubes and stored at -80°C until processing. The media was concentrated with a Centricon-10 Concentrator (contains a 10,000 MW cut-off, Amicon), The concentrated sample (total volume of about 800 μl to 1 ml) was transferred to an eppendorf tube on ice, then chromatographed on a desalting column (Bio-Rad). To reduce serum albumin (SA) levels, samples were chromatographed on an affi-gel blue (Bio-rad) column. The eluate was collected on ice after the sample absorbed into the column (1.5 to 2.0 ml). The protein concentration of an aliquot of the processed sample was determined using the DC Biorad protein assay (Bio-rad) with BSA as standard. The remainder of the sample was aliquoted and stored at -80°C.

5.6. Flow cytometry (FACS analysis)

Six to nine plates of confluent cells (100 mm plates) were harvested by treating each plate with 2.5 mM EDTA in HBSS (Hanks' balanced salt solution, Gibco) for 1-2 minutes at 4°C, adding 5 ml of FACS buffer (10% FBS in HBSS), and gently pipetting to lift the cells off the substratum. The cells were pelleted by centrifugation at 1200 rpm for 5 minutes, and resuspended in 6-7 ml (depending on the cell concentration) of

FACS buffer. An aliquot of the cell suspension was stained with trypan blue (0.4% in PBS) and the concentration of viable cells was determined to be between 80 and 90% using a hemocytometer and trypan blue exclusion (Harlow & Lane, 1988). Aliquots of $3x10^5$ cells were (7 aliquots per cell line analyzed) incubated with an anti-RHAMM antibody (2), nonspecific IgG, secondary antibody only, and no antibody at all. In preparation for staining, 2 ml of FACS Buffer was added to each tube, the cells pelleted by centrifugation at 1200 rpm for 5 minutes, and then resuspended in 200 μl of FACS buffer.

For staining, an aliquot of $3x10^5$ cells (in a total volume of 200 μl) was then incubated for 30 minutes on ice with a 1:100 dilution of the anti-RHAMM polyclonal antibody (R4). Negative control cells were incubated under the same conditions with a 1:100 dilution of rabbit IgG preabsorbed to mouse tissue (Sigma). To remove the excess antibody, the cells were washed once by adding 3 ml of cold FACS buffer, centrifuging at 1200 rpm for 5 minutes at 4°C, and then resuspending the cell pellet in 200 μl of cold FACS buffer. The fluorescein (FITC) labelled goat anti-rabbit IgG (GAR) antibody (Sigma) was added at a 1:20 dilution. The cells were then incubated for 30 minutes on ice with minimal light, and washed twice as described above. After the final wash, the cells were fixed by resuspending the cell pellet in 400 μl of freshly made 1% paraformaldehyde (Sigma) in PBS (pH 7.2), and

the samples were analyzed within a week using a Coulter Electronics EPICS 753 flow cytometer.

5.7. Immunofluorescence of cell monolayers

Cells were grown to confluence on sterile glass coverslips (previously rinsed in 85% ethanol and distilled water, and exposed to UV light for 3 hours to overnight to sterilize the surface) placed in 35 mm tissue culture plates. At confluence, the media was aspirated, the cells rinsed twice with PBS, and fixed for 10 minutes with (freshly prepared) 3% paraformaldehyde (Sigma) in PBS (pH 7.2). The cells were then subjected to three washes (10 minutes each) with wash solution (10% FCS/PBS containing 0.02% sodium azide), permeabilized with 0.2% Triton X-100/PBS for 3 minutes, and washed 3 more times. The cells were incubated overnight at 4°C with wash solution containing an anti-RHAMM polyclonal antibody (R4) (1:50 dilution) or an anti-vinculin monoclonal antibody (1:75 dilution, Sigma). Negative control cells were incubated with wash solution containing rabbit IgG (preabsorbed to mouse tissue) (1:50 dilution, Sigma) or mouse IgG (1:50 dilution, Sigma). The cultures were washed 5 times (10 minutes each) to remove excess antibody, and incubated with blocking solution (1 M Glycine in PBS) for 1 hour at room temperature to reduce autofluorescence. The cells were then incubated with tetramethylrhodamine isothiocyanate (TRITC) labelled goat anti-rabbit (GAR) or goat anti-mouse (GAM) IgG (1:300

dilution, Sigma) in wash solution for 3 hours at room temperature under minimal light conditions. After the cells were washed 5 times (10 minutes each) to reduce background staining, the coverslips were rinsed with 20 mM Tris-Cl (pH 7.2), followed by distilled water, and then carefully removed from the plates using forceps and a toothpick. The excess liquid was drained onto a kimwipe, and the coverslips mounted in "No Fade" Media (20 μl applied to the coverslip) (10 mM p-phenylenediamine, 118 mM Tris-HCl, pH 7.4, 90% glycerol) onto glass slides and the edges sealed with nail polish. The cells were viewed and photographed under a Zeiss Axiovert 35 mm fluorescent microscope the following day in order to minimize fading.

(6) Cell Behavior

6.1. Nuclear overlap ratio/Quantification of cell social behavior

To quantify loss of contact behavior, nuclear overlap ratios were obtained as described by Weston and Hendricks (1972). In determining the ratios, cells were grown to confluence in 60 mm tissue culture plates, then fixed and stained using a Leukostain Kit (Fisher Scientific). The number of nuclear overlaps were counted, using a 40X objective with a reticule containing a 20 x 20 grid, and a ratio calculated from these values (Weston and Hendricks, 1972). The nuclear overlap ratio of each cell line analysed was

determined 4 times. Student unpaired T-tests were used to statistically compare the ratios (n=4) between cell lines.

6.2. Loss of contact inhibition

A) Focus formation

Cell cultures grown past confluence were used to qualitatively examine foci formation in monolayer cultures. The overgrown cultures were obtained by growing the cells to confluence in 60 mm plates, and then replenishing the medium every 3 days (at least twice) to allow for further growth. To observe focus formation, the overgrown cultures were fixed and stained (Leukostain Kit), and the underside of the plates examined.

B) Saturation density

To determine the cell densities of cultures described above, cells were harvested from a 60 mm plate with trypsin (0.25%)-EDTA (2 mM), washed by centrifugation, and the cell pellet resuspended in 3 ml of growth medium. An aliquot of the cell suspension was stained with trypan blue (0.4% in PBS) and the concentration (cells/ml) of viable cells determined using a hemocytometer and trypan blue exclusion (Harlow & Lane, 1988).

6.3. Timelapse analysis of cell motility

Motility assays were conducted using a computerized timelapse image analysis system (Image-I, Universal Imaging Corporation, Westchester, PA) capable of quantifying random locomotion by measuring nuclear displacement. For the motility experiments in which the parental 10T½ cells were screened for their ability to consistently display the phenomenon of contact inhibition of movement (Abercrombie *et al.*, 1970), cell locomotion was daily examined until confluency was reached. In preparation for this analysis, $4x10^5$ cells were seeded into a 25 cm^2 tissue culture flask (Corning), containing 5 ml of growth medium (10% FCS/DMEM, Hepes, pH 7.2). The cells were filmed under a 10X microscope objective lens (Model. IM35; Zeiss), and the rate of movement daily determined by tracking the cells every 20 minutes for a 2 hour period, starting a day after subculture and continuing until confluence (24 hour (h), 48h, 72h, 96h). The motility analysis was performed in triplicate. To analyze the data, the velocities of the 3 experimental groups were pooled and Student Unpaired T-tests were used to statistically compare the total data obtained for the 24 hour (h) time to the total data obtained for each of the subsequent times after subculture (48h, 72h, 96h).

For the motility studies which focused on confluent cultures (RHAMM transfected and control cells), cells were grown to confluence in tissue culture flasks containing 5 ml

of growth medium (as above). The cells were filmed under a 40X objective lens and the motile rates determined by tracking the cells every 20 minutes for a 2 hour period.

6.4. *In vivo* tumor studies

Confluent cell cultures (about 80% confluent) were harvested using trypsin-EDTA (as in Cells and Culture), washed by centrifugation, and resuspended in PBS to determine the cell concentration (cells/ml). Three hundred thousand cells, in a total volume of 0.5 ml of PBS, was subcutaneously injected into the scapular region of male C3H mice (6-8 weeks old). Five mice were injected with each RHAMM transfectant (Clone 6, Clone 10 and Clone 12), and control cells (control vector and *ras*-transformed C3 cells). Tumor growth was monitored and detected by palpitation. The mice were sacrificed and the dissected tumors processed for histological analysis.

6.5. Metastasis assay

An experimental metastasis assay (Egan *et al.*, 1987; Damen *et al.*, 1989) was used to assess the metastatic potential of the cells *in vivo*. For this, cells were grown to confluence in 100 mm tissue culture plates and harvested by treating the cells with 3 ml of 2.5 mM EDTA in HBSS, for 1-2 minutes at 4°C. Five ml of growth medium (10% FCS/DMEM, 10 mM Hepes, pH 7.2) was added, and the solution gently pipetted to

lift the cells off the surface. The cells harvested from 6-8 plates were pooled, pelleted by centrifugation at 1200 rpm for 5 minutes at room temperature, and resuspended in 3-5 ml (depending on the concentration of cells harvested) of HBSS. An aliquot of the cell suspension was stained with trypan blue (0.4% in PBS) and the concentration of viable cells was determined using a hemocytometer and trypan blue exclusion (Harlow & Lane, 1988). The cells were centrifuged in HBSS to wash away any FCS remnants, and the sample was resuspended in HBSS.

Three hundred thousand cells, in a total volume of 0.2 ml, were injected into the tail veins of female C3H mice (about 6-8 weeks old). Five mice were injected for each cell line assayed. Prior to the injections, the mice were prewarmed under a heating lamp for 5 minutes, in order to dilate the vein. Three to twelve weeks after the injections, the animals were sacrificed by overexposure to carbon dioxide. Lungs were fixed by intratracheal injection with 10% neutral buffered formalin (4 g NaH_2PO_4, 6.5 g Na_2HPO_4 (anhydrous), 900 ml distilled water, 100 ml 37% formaldehyde), dissected out, and stored in the fixative overnight at room temperature. The lungs, displaying metastatic nodules, were stained by immersion in Bouin's solution (picric acid, formaldehyde, acetic acid [15:5:1]) for 3 hours, and then stored in 70% ethanol. The number of tumors on the lung were counted under a dissecting microscope, and slides were prepared for

histological analysis.

6.6. Micrometastasis

To detect micrometastasis in the lungs, mouse tail vein injections were performed on C3H female mice as previously described (Metastasis assay) and the lung explants cultured under sterile conditions (Gingras *et al.*, 1990) at two and twelve weeks post-injection. For the preparation, each lung explant was prepared immediately after the mouse was sacrificed by carbon dioxide overdose. The lung was aseptically dissected out of the mouse, rinsed with PBS containing 5X pen-strep (penicillin - 500 units/ml, streptomycin sulphate - 500 μg/ml) and cut into small fragments. The lung sections were manually homogenized in a polypropylene tube containing 0.5 ml of growth medium (10% FCS/DMEM containing 10 mM Hepes, pH 7.2 , and 1X pen-strep), and the volume of the lung suspension was then brought up to 10 ml with the same medium. The sample was kept at room temperature for about 10 minutes to allow the large particles to settle to the bottom of the tube. Each lung was then explanted into two 100 mm tissue culture plates by combining 5 ml of the homogenate with 5 ml of growth media. The cultures were incubated at 37°C under 5% CO_2, and 24 hours later the medium of one of the plates was replenished with normal growth medium, and the other one with growth medium supplemented with geneticin (0.6 mg/ml, Gibco). From then on

the medium was changed every 3 days and the cell growth from the explant daily monitored for approximately 4 weeks. Micrometastasis was detected as cell growth resistant to geneticin. For the primary cultures, in which the cells grew to about 75% confluence in the absence of geneticin, the cells were harvested and split into 2 tissue culture plates containing geneticin media. Additionally, when cells reached a similar state of confluence in the presence of geneticin, the cells were passaged and subjected to further growth in geneticin media. The cells were passaged in geneticin several times to ensure that cells containing the neomycin resistance gene were being selected.

RESULTS

1. 10T½ cells displayed contact inhibition of movement

Mouse 10T½ fibroblasts were selected as the immortalized cell line to be used in the RHAMM cDNA transfection studies because they exhibit strong contact inhibited behavior in culture (Butler, 1991; Alberts *et al.*, 1989), and since much of the previous work with RHAMM utilized 10T½ derived cell lines (Turley *et al.*, 1989; Turley *et al.*, 1991; Hardwick *et al.*, 1992; Samuel *et al.*, 1992; Samuel *et al.*, 1993; Turley, *et al.*, 1993). Furthermore, this cell line was not prone to spontaneous transformation like NIH 3T3 cells (Egan *et al.*, 1987).

The characterization of the 10T½ cell line in terms of motile behavior, involved daily examination of its rate of random locomotion with image analysis, starting a day after subculture and continuing until the cells reached confluence (96 hours or 4 days). Analysis of the data showed a motility decline in parallel with growing confluence, which was significant (Student unpaired t-tests) when the cells reached confluence (Figure 4). The decreased motility rates were a measure of contact inhibition (Abercrombie, 1970), and thereby demonstrated that the 10T½ cell line was an appropriate system for investigating the molecular mechanisms underlying this phenomenon.

2. Construction of a RHAMM ß-actin pHßApr1-neo Expression Vector

A RHAMM II cDNA (exons 6-14) (Hardwick *et al.*, 1992) was obtained by ligating the restriction fragments of two partial RHAMM cDNAs (1.7 kb and 1.9 kb), which had been originally isolated from a λgt11 mouse 3T3 library and amplified in Bluescript (Hardwick *et al.*, 1992). Restriction analysis of the purified plasmid DNA, confirmed that the ligation of the cDNA fragments and their insertion into the plasmid, had occurred in the correct orientation. In particular, doubly digesting the recombinant plasmids with the enzymes used to initially construct the RHAMM cDNA (described in methods), generated restriction fragments which comigrated with the purified parental fragments (i.e. 1.1 kb and 1.5 kb) on an agarose gel (Figure 5).

In order to insert the full length RHAMM II cDNA into the correct frame of the ß-actin expression vector, the cDNA was amplified by PCR using the recombinant RHAMM Bluescript plasmid as the template. A complete 2.9 kb RHAMM cDNA, encoding exons 6 to 14 (not produced by ligations, but isolated from the λgt11 stock), was used as a control template for the PCR reaction. Since both PCR products, the ligated and 2.9 kb RHAMM cDNA, yielded a 1.7 kb fragment after Sal I and Hind III digestion, this further confirmed that the correct insert (RHAMM II cDNA) was amplified (data not shown).

The Sal I-Hind III RHAMM cDNA fragment was then ligated

into the ß-actin expression vector (pHßApr1-neo) and amplified in HB101 bacteria. Colonies containing the expression vector were selected by ampicillin resistance and colony hybridisation to the radiolabelled RHAMM cDNA (partial 1.7 kb) probe. Digestion of the purified recombinant with Sal I and Hind III, generated the specific 1.7 kb fragment, and thereby further confirmed that the vector contained the RHAMM II cDNA insert (Figure 6).

3. RHAMM II (exons 6-14) was overexpressed in 10T½ cells

10T½ fibroblasts were transfected by lipofection with the RHAMM II cDNA (exons 6-14) in the expression vector containing a ß-actin promoter and a selectable neomycin resistance gene (Figure 3) (Gunning *et al.*, 1987). The parental cells, transfected with the empty vector, served as controls. Stable transfectants were selected in G418, and at least 30 clones were picked and expanded as cell lines. Cloned cell lines overexpressing the RHAMM protein were identified by western analysis of the confluent cell lysates. Three clones, one overexpressing the RHAMM protein by four fold (Clone 12), and the other two expressing varying levels of the protein (Clone 6 and Clone 10), were then subjected to further analysis (Figure 7). Since transfection studies with a RHAMM IV4 cDNA and genomic DNA were being performed at this time to confirm results present here (Hall *et al.*, submitted), this analysis examined 3 clones exhibiting varying expression of the RHAMM

protein.

The RHAMM protein expression, in cells derived from confluent cultures, was determined by immunoblot analysis of the cell lysates, using an anti-RHAMM polyclonal antibody generated against a peptide sequence encoded in the cDNA. The anti-RHAMM polyclonal (against amino acids 125-145) (Hardwick *et al.*, 1992) detected a protein of MW 86 kDa, and densitometric analysis indicated that Clone 12 cells overexpressed the RHAMM protein by four fold relative to the empty vector controls (Figure 7). Since the cDNA was predicted to encode a 52 kDa protein, the detection of a larger protein likely represented a glycosylated form.

The stable integration of the transfected RHAMM cDNA (1.7 kb) into the 10T½ cells' genome was confirmed by PCR amplification of the cDNA, using primers from the vector arms and transfected cells' DNA as the template. The radiolabelled RHAMM cDNA probe detected the specific 1.7 kb fragment in the PCR products of the Clone 10 and Clone 12 samples, but showed no presence in the control vector's product (data not shown). The failure to detect the DNA fragment (1.7 kb) in the control vector cells was consistent with the cells being transfected with the expression vector alone, and the fact that PCR could not amplify the cells' genomic RHAMM, which spans approximately 25 kb (Entwistle *et al.*, submitted).

Northern blot analysis, using a radiolabelled RHAMM cDNA as a probe and RNA extracted from confluent cultures of RHAMM

transfected and empty vector control cells, revealed a weak 1.7 kb band, as well as a 4.2 kb band which was slightly elevated in Clone 12. Reverse transcriptase PCR (RT-PCR) amplified a 0.76 kb message that was present in greater amounts in Clone 12 than control vector cells (or Clone 10) (Figure 8).

4. RHAMM II (exons 6-14) transfected cells failed to overexpress RHAMM in the extracellular milieu

To determine if the RHAMM II cDNA transfections led to an alteration in the amount of RHAMM protein secreted by the cells, the media of confluent cultures was collected. Immunoblot analysis, using the anti-peptide antibody, showed that Clone 10 and Clone 12's production of soluble RHAMM was not elevated above control cells (data not shown). This indicated that the protein overexpressed was not secreted.

5. RHAMM was localized by immunofluorescence in cells overexpressing this protein

FACS analysis was conducted to determine if the RHAMM II transfected 10T½ cells exhibited an increase in membrane expression of this protein as predicted (see introduction). The results indicated that the RHAMM II transfected cells (Clone 12) displayed elevated levels of RHAMM on the cell surface (Figure 9).

Immunofluorescent analysis of Clone 12 (Figure 10C)

confirmed that in confluent cell cultures RHAMM was markedly increased relative to the control cells (Figure 10A,B). Additionally, while the control vector and parental cells' staining for RHAMM appeared to be fibrillar in the cytoplasm, the RHAMM transfected cell line displayed a more diffuse granular staining pattern throughout the cell. Furthermore, RHAMM transfected cells showed elevated aggregated staining for RHAMM in the nucleus (Figure 10C). Specific RHAMM staining was indicated by the lack of stain observed in the control cells incubated with rabbit IgG preabsorbed to mouse tissue (Figure 10D).

6. RHAMM II (exons 6-14) transfected cells morphologically resembled transformed cells and showed a loss of contact inhibition

The morphology of the cells (Clone 12) containing a four fold increase in the RHAMM protein (exons 6-14) resembled that of transformed cells (Figure 11i,j) (Porter *et al.*, 1973; Alberts *et al.*, 1989). Control cells (10T½ and vector) (Figure 11a,b, c,d) and Clone 6 (Figure 11e,f) displayed normal contact inhibited behavior (no nuclear overlapping). The Clone 10 cells (Figure 11g,h) exhibited narrow cellular processes, and although there was no obvious nuclear overlapping, the nuclei of adjacent cells' appeared to be in closer proximity than that of controls. This altered behavior morphology was not reflected in changes in the nuclear overlap

ratio. The most dramatic phenotypic effect was observed for the Clone 12 cells which exhibited the highest overexpression of the RHAMM protein. The Clone 12 cultures appeared morphologically disorganized with obvious displays of nuclear overlapping. These observed effects were confirmed by significantly increased nuclear overlap ratios (Figure 12). Indeed, the ratio for Clone 12 was found to be similar to the *ras*-transformed cells (C3). Furthermore, statistical analysis (using student unpaired t-tests) indicated that the ratios for C3 and Clone 12 were significantly greater than the vector only controls (Figure 12).

7. Clones overexpressing RHAMM II (exons 6-14) formed foci in monolayer cultures

Consistent with the observed changes in morphology, the cells overexpressing the RHAMM II protein formed foci, to varying degrees, in monolayer cultures grown passed confluence (Figure 13). In particular, Clone 12's (Figure 13, #5) ability to form multiple foci resembled *ras*-transformed (C3) cells (Figure 13, #2). Vector only controls did not form foci (Figure 13, #1). To further assess the loss of contact inhibition, the density to which the cells grew, was determined as shown in Figure 14. Since the density of Clone 12 cells was greater than controls, this was indicative of their ability to overcome the normal constraints on cell division, and further confirmed the cells loss of contact

inhibition.

8. RHAMM II (exons 6-14) overexpressing cells displayed reduced focal adhesions

Focal adhesions have been implicated in contact behavior and RHAMM has been shown to regulate focal adhesion turnover (Burridge, 1988; Hall *et al.*, 1994). The activation of the RHAMM receptor was found to elicit signal transduction events which included transient tyrosine phosphorylation that occurred within focal adhesions, followed by a prolonged dephosphorylation event that corresponded with disassembly of these units. To further assess the relationship between RHAMM and focal adhesions, these sites were examined using an antibody to a protein (vinculin) typically found there. The focal adhesion formation of all the RHAMM transfected cells appeared to be disrupted (Figure 15). The parental 10T½ (A) and control vector (B) cells stained vinculin as elongate punctate stains, and Clone 12 cells (D) displayed vinculin as thinner punctate patterns. Although the overall number of focal adhesions was not greatly reduced in Clone 12, the finding that it stained vinculin somewhat less intensely than control vector and parental 10T½ cells, was indicative of altered focal adhesion structure. Clone 6 cells exhibited both punctate and aggregate staining of vinculin (not shown). Although, the punctate staining appeared to be slightly shorter than that of the control cells, the focal contacts

observed in this clone was most similar to the contact inhibited control cells. In the Clone 10 cells (C), the vinculin primarily occurred as intensely stained aggregates. Mouse IgG controls (nonimmune IgG) showed no staining.

9. RHAMM II (exons 6-14) transfected cells did not display an increase in cell locomotion

In examining how RHAMM overexpression affects cell locomotion, cells from confluent cultures were subjected to motility studies using timelapse analysis. The results showed no significant difference between the motile rates of Clone 12 and control vector cells (Table 1).

10. Clones overexpressing RHAMM II (exons 6-14) were not tumorigenic *in vivo*

To evaluate RHAMM's tumor forming ability *in vivo*, transfected cells were subcutaneously injected into mice. While the *ras*-transformed (C3) cells produced tumors within 3 weeks, the RHAMM transfected cells failed to generate tumors even after 5 months.

11. RHAMM II (exons 6-14) transfected cells did not form metastasis in the lung

Additionally, transfected cells were subjected to a lung colonization assay after tail vein injections into mice. At 3 weeks post injection, the mice injected with the positive

control *ras*-transformed (C3) cells, formed metastasis. However, since the mice injected with the RHAMM transfected cells (Clone 10, and Clone 12) appeared healthy, they (along with the control mice injected with the vector and 10T½ cells) were not sacrificed at this time. After 3 months, no metastasis was observed in the parental 10T½ (Egan *et al.*, 1987a), empty vector control cells, Clones 6, 10 or 12.

Although RHAMM transfected cells were not able to form tumors, we hypothesized whether they were capable of initially invading the lungs. Therefore, to investigate RHAMM's potential role in microinvasion of the lung, RHAMM transfected cells (Clone 10 and Clone 12) were injected into the tail vein of mice, and after 12 weeks the lungs were explanted into culture. To validate culture conditions, *ras*-transformed (C3) cells were injected into separate mice, the lungs collected and cultured as above. In these assays, G418 resistant cells were obtained. Since the empty vector controls, the parental cell line, and Clones 6, 10, and 12, failed to form cell growths, these results indicated that these cells had not invaded the lungs.

FIGURE 4. 10T½ cells displayed contact inhibition of movement. The mean cell velocity was determined at various times after subculture. The * (96 h) signifies that the motile response was significantly different from the 24 h time (Student unpaired t-tests). Values represent the mean±SE of n=60 cells.

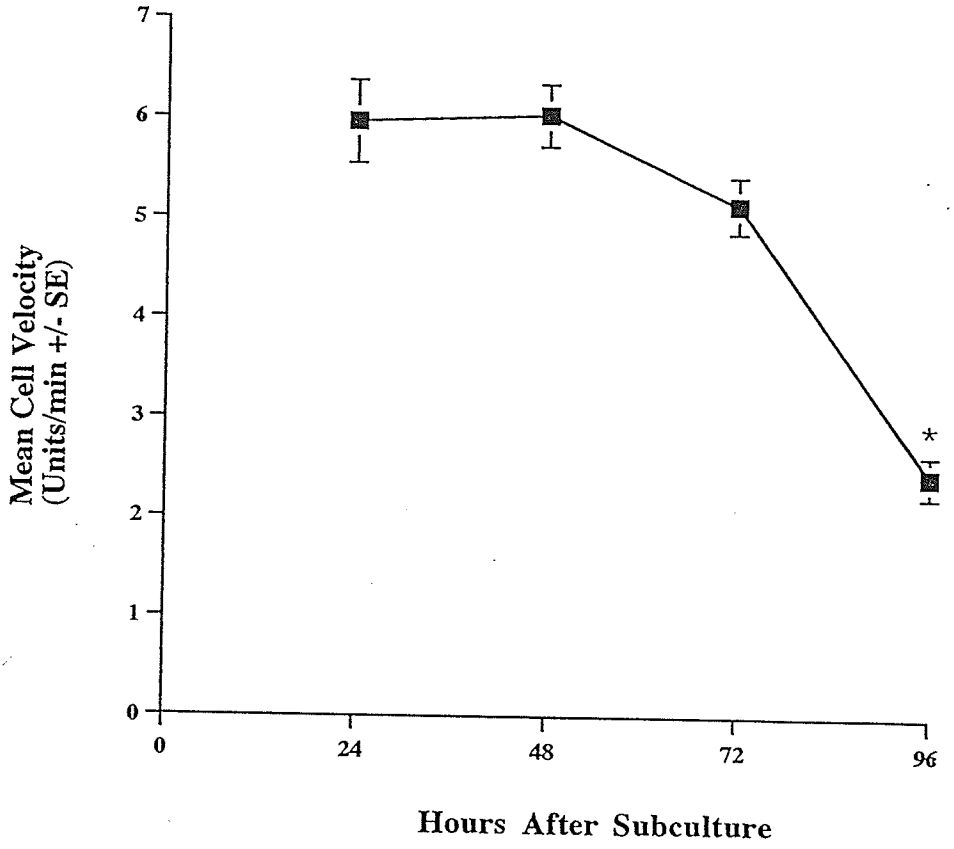
Mean Cell Velocity
(Units/min +/- SE)
7
6
5
4
3
2
1
0
0
24
48
72
96
*
Hours After Subculture

FIGURE 5. Restriction analysis indicated that the ligation of the partial RHAMM cDNAs occurred in the correct orientation. Restriction fragments of partial RHAMM cDNAs were ligated together, amplified in Bluescript, and the purified plasmids doubly digested with Eco RI-Bgl II (Lane 4), and Sac I-Bgl II (Lane 5). The restriction fragments comigrated with the corresponding parental RHAMM cDNAs obtained by digestion with Eco RI-Bgl II (Lane 2) and Sac I-Bgl II (Lane 1). The digested Bluescript plasmid (opened) was run as a control (Lane 3). Restriction fragments were analysed on 1% agarose gels.

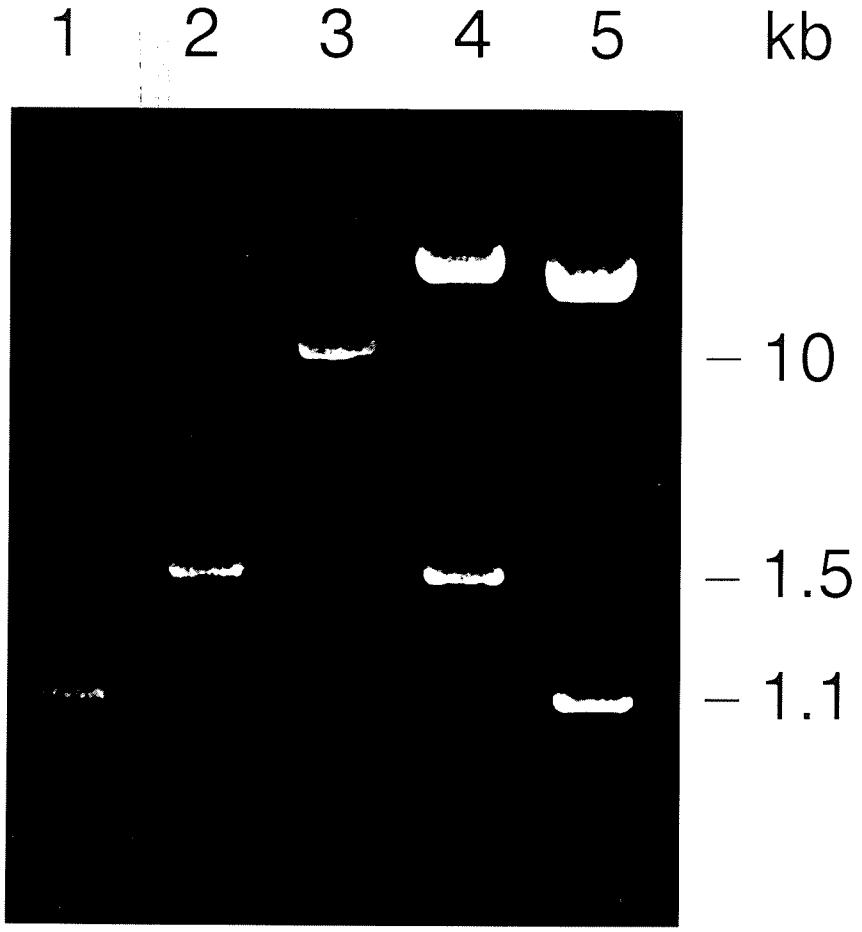
1
2
3
4
5
kb
10
1.5
1.1

FIGURE 6. ß-actin expression vector contained the RHAMM II cDNA (exons 6-14) insert. The RHAMM cDNA reading frame was amplified by PCR for insertion into the expression vector. The recombinant vector containing the ligated RHAMM II cDNA was amplified in bacteria (HB101) and selected by drug resistance (ampicillin) and colony hybridization to a RHAMM cDNA (1.7 kb) probe. Sal I-Hind III digestion of the purified plasmid yielded a 1.7 kb fragment (Lane 2), as did the control (Lane 1). The control sample represented a Sal I-Hind III digestion of the complete RHAMM cDNA (exons 6-14) (purified from a λgt11 stock) which was also amplified by PCR for insertion into the expression vector. Restriction analysis was performed on 1% agarose gels.

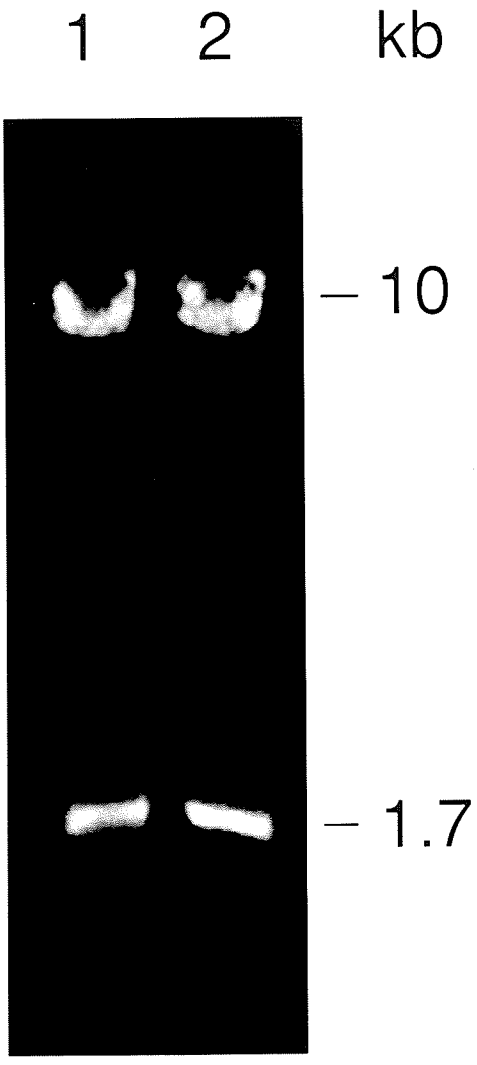
1
2
kb
10
1.7

FIGURE 7. Immunoblot analysis of RHAMM protein expression in transfectants. The clones and control cells were grown to confluence, and lysates prepared using RIPA buffer. 10 μg of total protein was electrophoresed on SDS-PAGE gels, transferred onto nitrocellulose and immunoblotted using an anti-RHAMM polyclonal antibody (R4). The clones analysed included Clone 6, Clone 10, and Clone 12 (Lanes 1, 2, and 3). Control cells included untransfected 10T½ cells, vector transfected cells, and *ras*-transformed cells (Lanes 4, 5, and 6). Clone 12 displayed overexpression of the RHAMM protein.

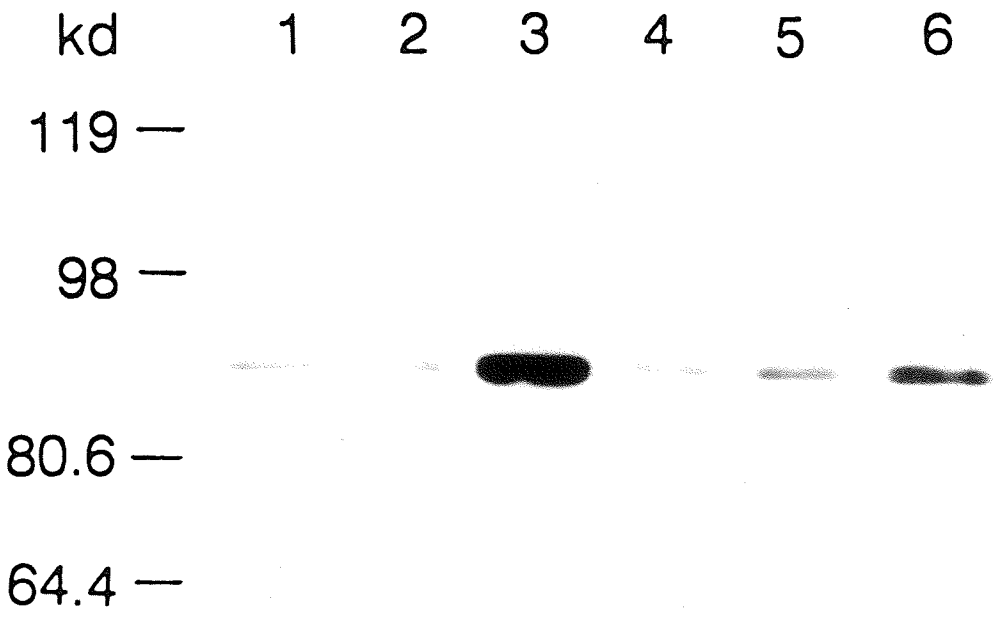
kd
1
2
3
4
5
6
119
98
80.6
64.4

FIGURE 8. Amplification of the RHAMM II cDNA transcript in cells overexpressing the RHAMM protein. Reverse transcriptase PCR amplified a 0.76 kb fragment that was present in elevated levels in Clone 12 (Lane 3) and reduced levels in untransfected 10T½ (Lane 1) and control vector cells (Lane 2). RNA-ase treated cellular RNA is shown in Lane C and ß-actin loading controls are shown in the lower panel.

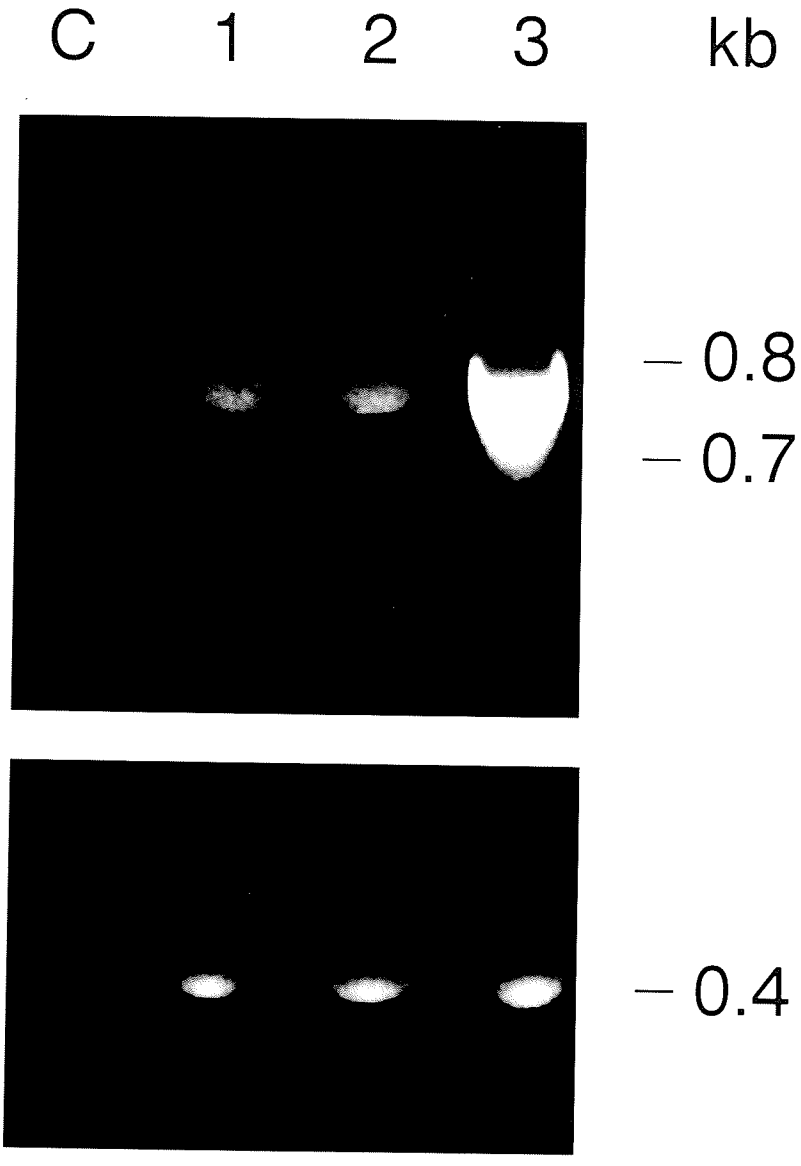
C
1
2
3
kb
0.8
0.7
0.4

FIGURE 9. RHAMM transfections increased RHAMM membrane expression. Cells, transfected with a RHAMM cDNA containing a mutated HA binding domain, were harvested from confluent cultures and labelled for RHAMM using a polyclonal antibody (R4) and fluorescein-labelled secondary antibody (GAR-FITC). Control cells were stained with rabbit IgG (preabsorbed to mouse tissue). Cells were washed, fixed and analyzed on a Coulter Flow Cytometer. Shown are fluorescence profiles of control vector and three transfected clones (4D, 5B, and 5C). These results indicate that RHAMM II (exons 6-14) can also be targetted to the cell surface.

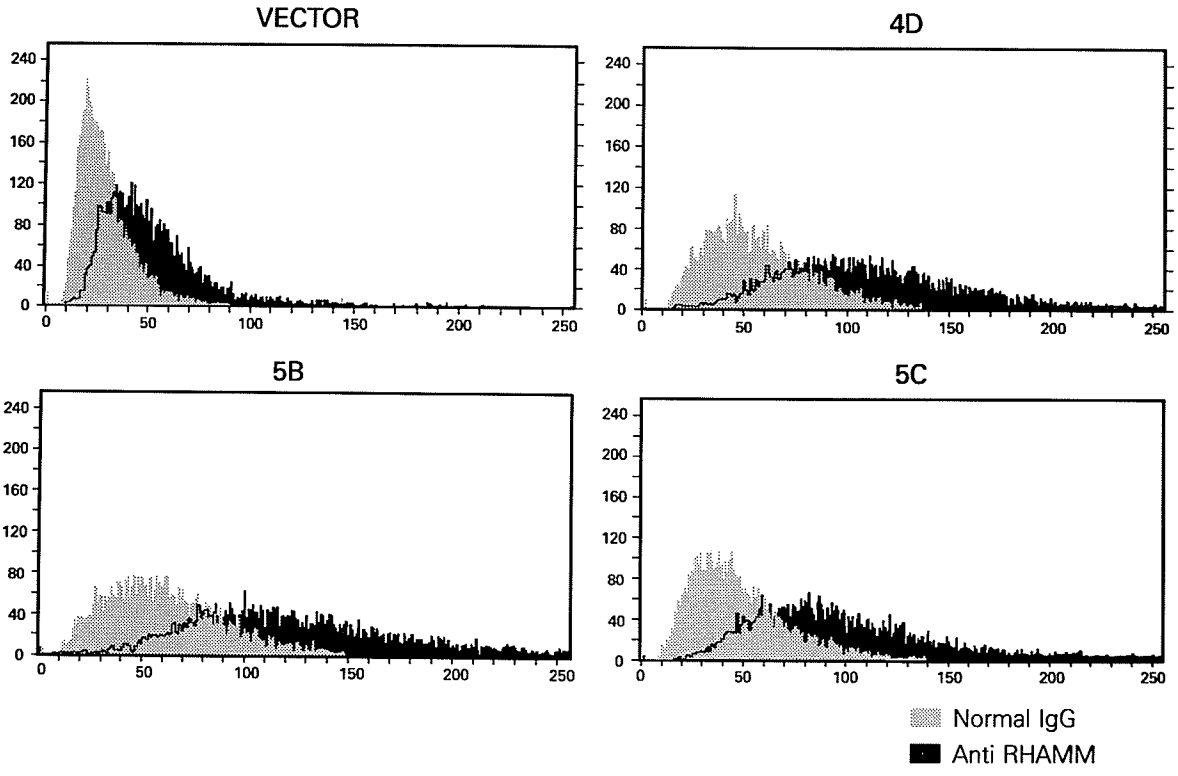
VECTOR
4D
5B
5C
240
200
160
120
80
40
0
0
50
100
150
200
250
Normal IgG
Anti RHAMM

FIGURE 10. RHAMM overexpressing cells showed increased protein expression intracellularly. Confluent cell cultures were fixed and the intracellular RHAMM distribution in (A) untransfected 10T½, (B) control vector, and (C) Clone 12 cells detected with an anti-RHAMM polyclonal antibody (R4) and a fluorescein labelled secondary antibody (GAR-FITC). (D) Control cells were incubated with rabbit IgG (preabsorbed to mouse tissue). The scale bar represents 50 microns (630X magnification).

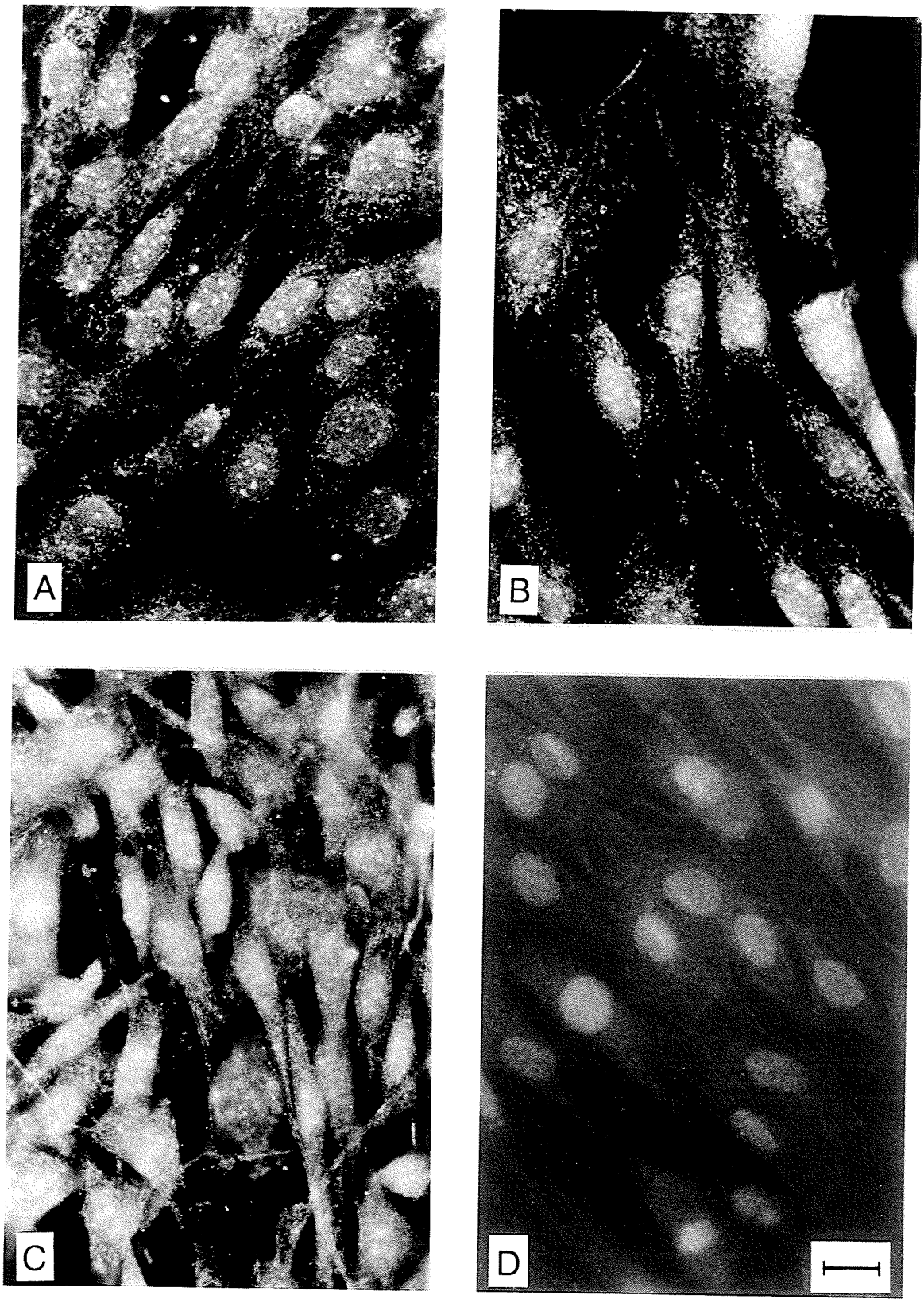
A
B
C
D

FIGURE 11. RHAMM overexpressing cells exhibited morphological changes resembling transformed cells. Photomicrographs illustrate morphological differences between (a,b) 10T½, (c,d) control vector, (e,f) Clone 6, (g,h) Clone 10, and (i,j) Clone 12. Confluent cell cultures were fixed, the nuclei stained, and photographed under a 10X (a,c,e,g, and i) and 40X (b,d,f,h, and j) objective lens.

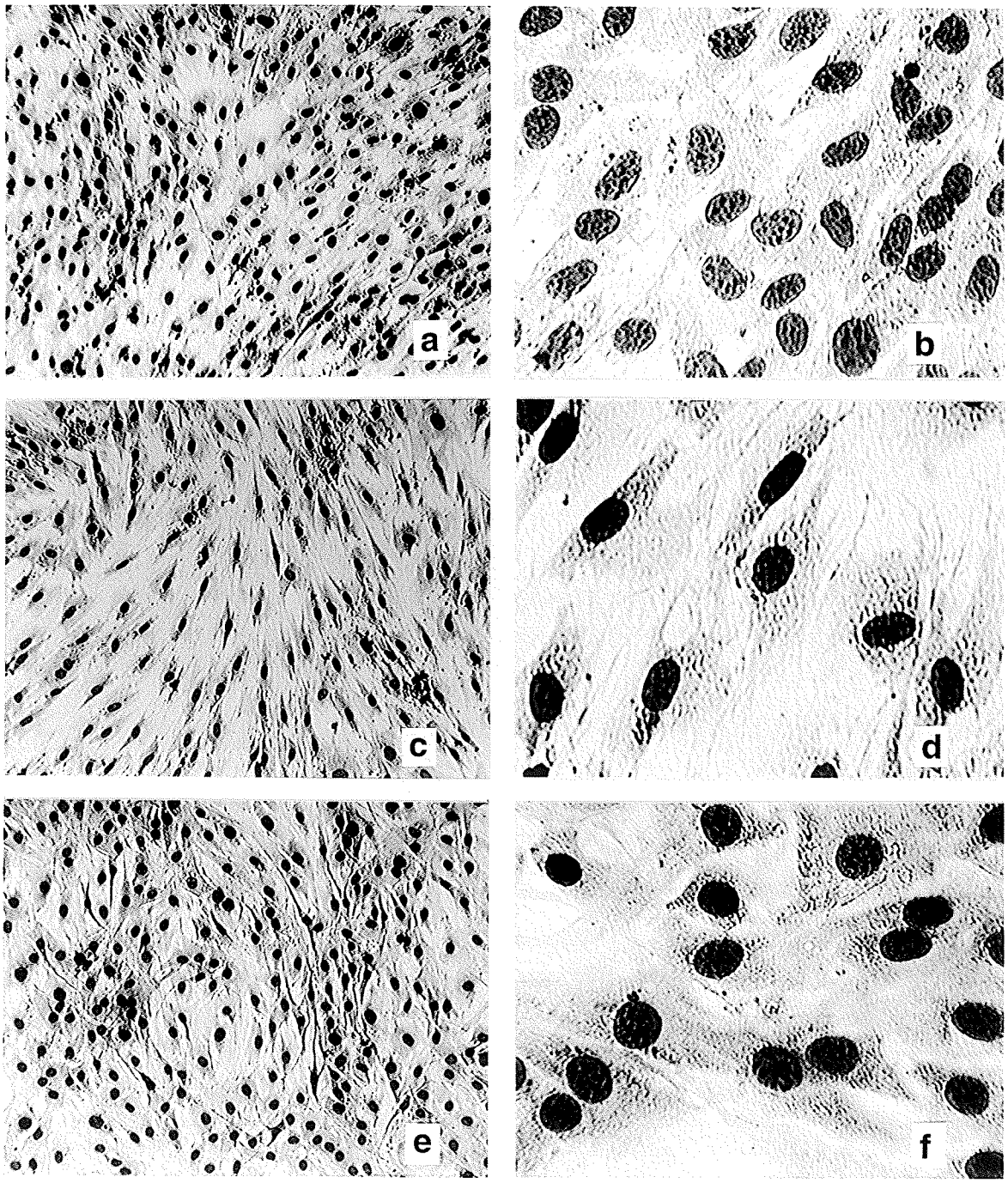
a
b
c
d
e
f

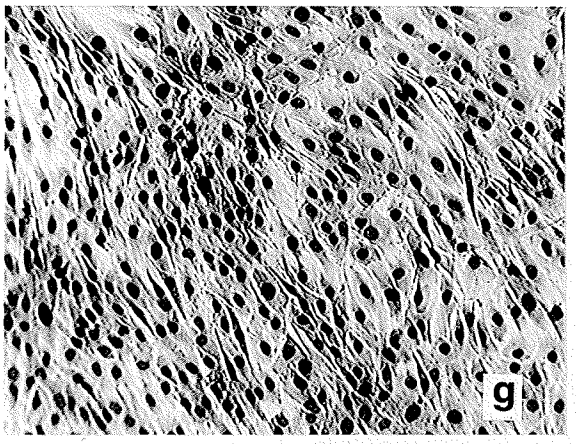
g

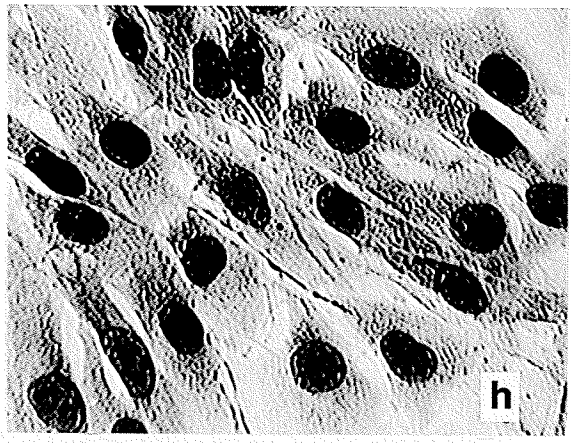
h

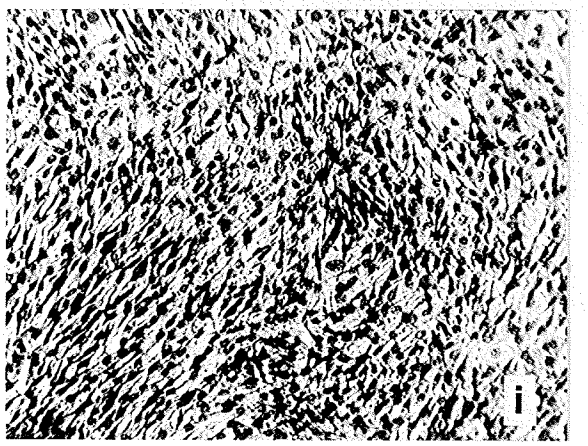
i

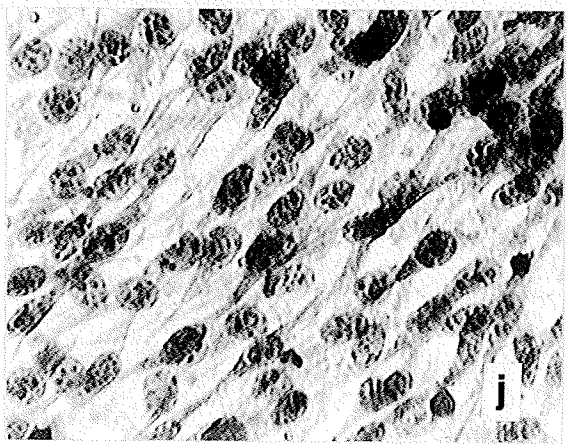
j

FIGURE 12. RHAMM overexpression affected nuclear overlap ratios. The nuclear overlap ratios of confluent cultures photographed in Figure 11 were determined as described by Weston and Hendricks (1972). The number of nuclear overlaps were counted and a nuclear overlap ratio calculated from these values. The values graphed represent the mean (n=4) and * indicates that *ras*-transformed (C3) and Clone 12 cells were significantly greater ($p<.001$) than control vector and untransfected 10½ cells.

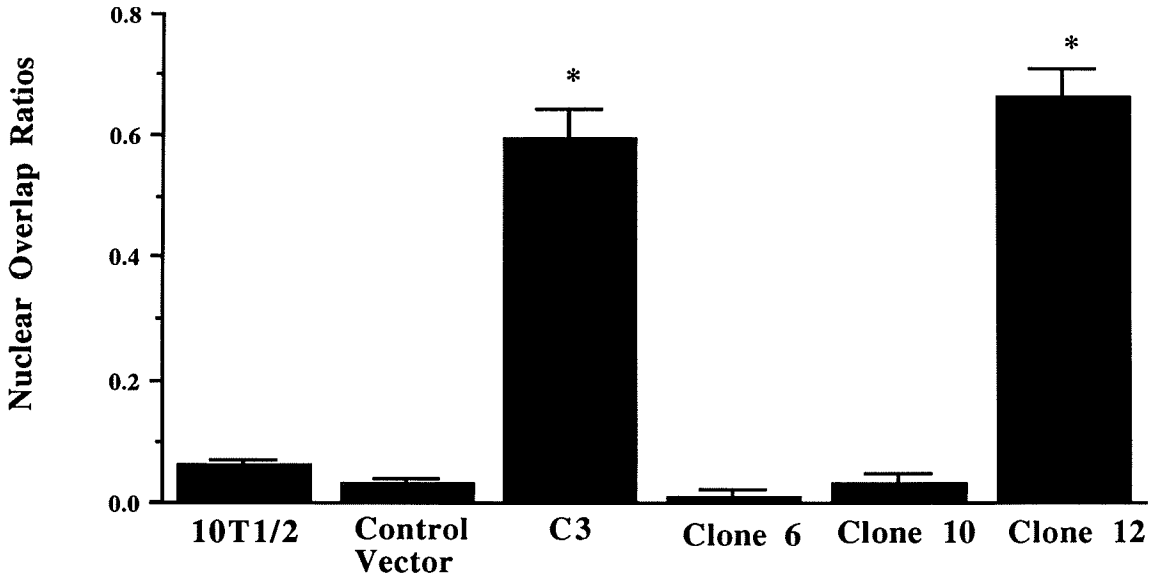
Nuclear Overlap Ratios
0.8
0.6
0.4
0.2
0.0
*
*
10T1/2
Control Vector
C3
Clone 6
Clone 10
Clone 12

FIGURE 13. RHAMM overexpression coincided with focus formation. Cells were grown to confluence, and the media was then replenished to allow for further growth. After the cell cultures were fixed and the nuclei stained, the underside of the plates were photographed. The darker areas represented increased nuclei staining and was indicative of cell piling up into multiple layers. (1) Control vector (2) *ras*-transformed (C3) (3) Clone 6 (4) Clone 10 (5) Clone 12. Clone 12 cells formed multiple foci like the transformed cells.

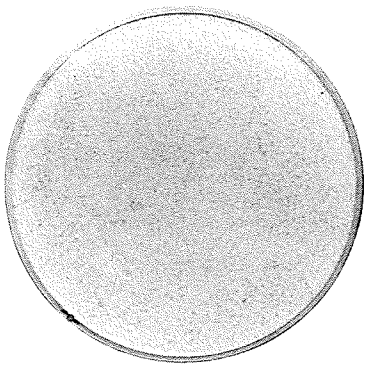

1

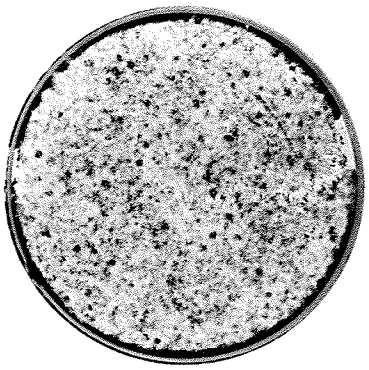

2

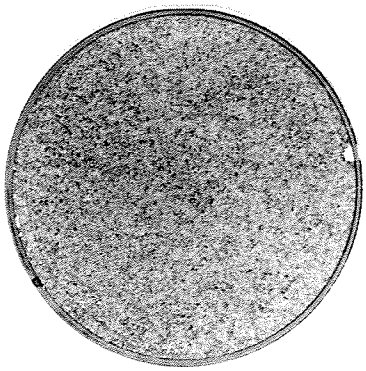

3

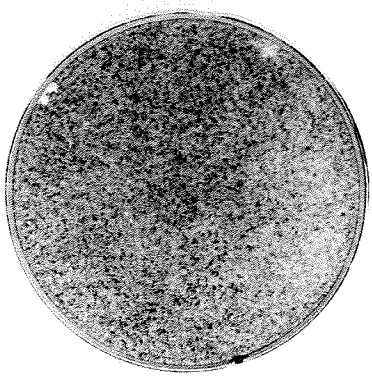

4

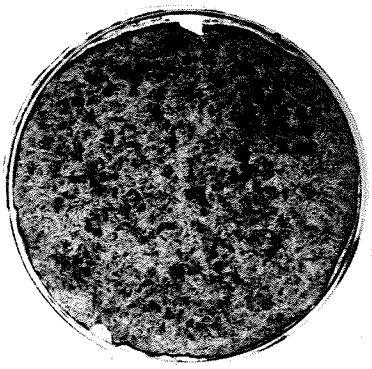

5

FIGURE 14. RHAMM overexpression corresponded with the cells' ability to overcome the normal constraints on cell division. The cell density (cells/ml) of cultures grown passed confluence (as in Figure 13) was determined. The values graphed represent the mean (n=3) ±SE. The cell density of *ras*-transformed (C3) cells was not included due to the cell lines' failure to form monolayer cultures like the clones and control cells. The Clone 12 cells' density was increased relative to the untransfected 10T½ and control vector cells.

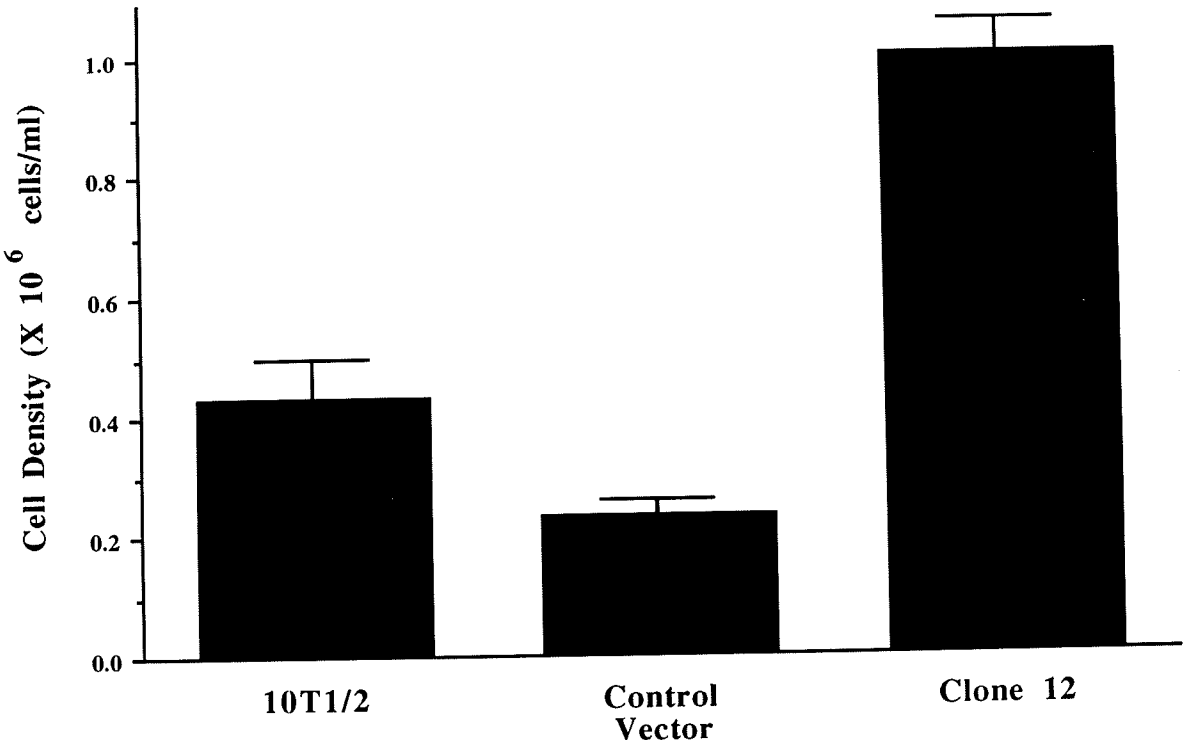
Cell Density (X 10 6 cells/ml)
1.0
0.8
0.6
0.4
0.2
0.0
10T1/2
Control Vector
Clone 12

FIGURE 15. RHAMM transfectants displayed altered focal adhesions. Confluent cell cultures were fixed and stained for vinculin using a monoclonal antibody and a fluorescein labelled secondary antibody (GAM-TRITC). The (A) untransfected 10T½ and (B) control vector cells' showed elongate punctate staining for vinculin. (C) Clone 10 exhibited nodular stains and (D) Clone 12 thin punctate stains. (E) Control cells were incubated with nonspecific mouse IgG. The scale bar represents 50 microns (630X magnification).

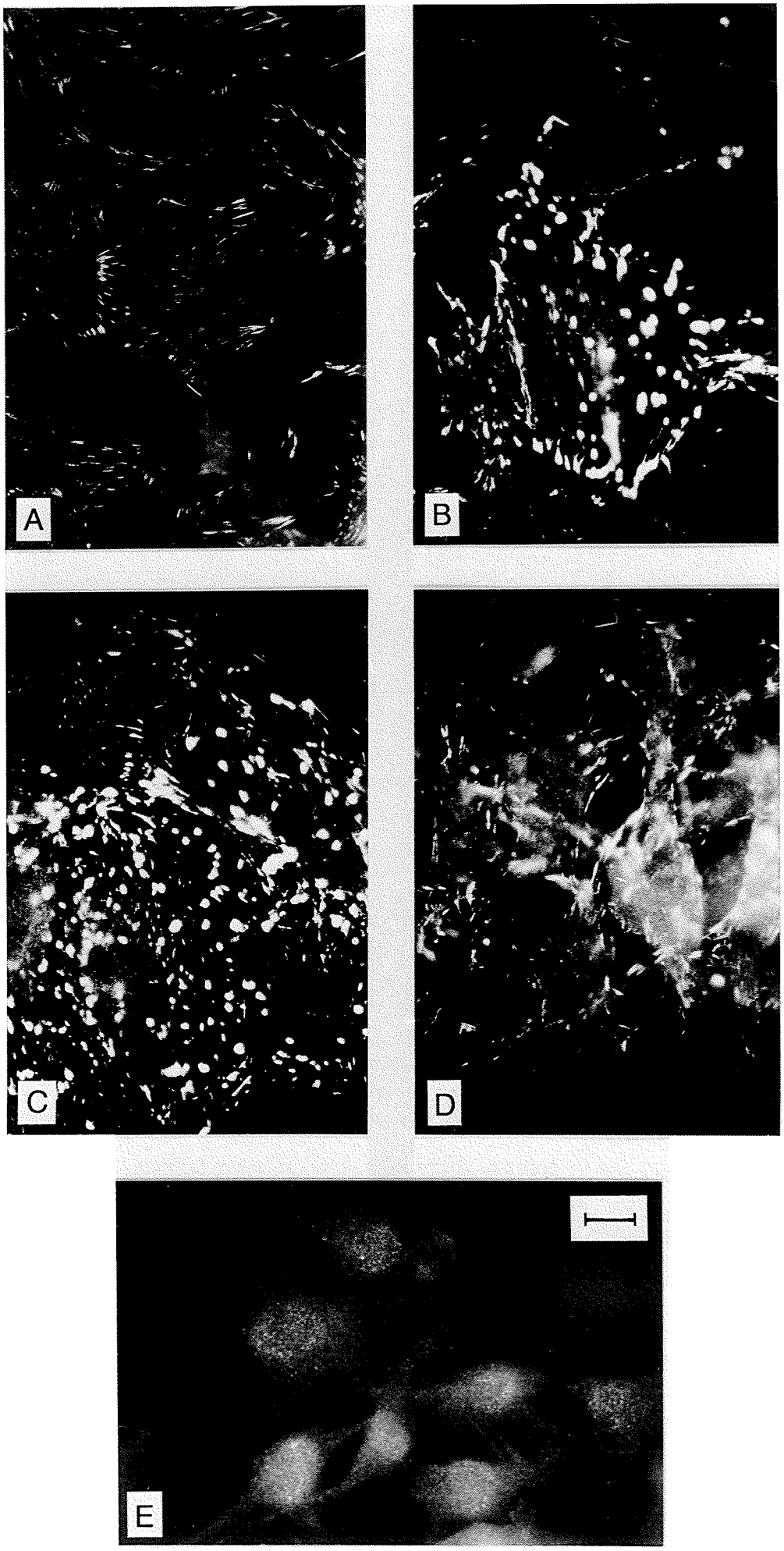
A
B
C
D
E

Table 1. Motile rates of RHAMM overexpressing cells was similar to control cells.

Trial	Motile Rates of Cells (Units/min.)	
	Control vector transfected	Clone 12
1	4.10	3.86
2	3.94	4.00
3	3.90	3.83
4	3.80	3.76
5	3.96	3.91

A computerized timelapse image analysis system was used to determine the motile rates of control vector transfected and RHAMM overexpressing (Clone 12) cells. Cells of confluent cultures were filmed under a 40X objective lens, and tracked every 20 minutes for a 2 hour period.

DISCUSSION

This study examined the effects of RHAMM II (exons 6-14) (Hardwick *et al.*, 1992) overexpression in normal contact inhibited cells. We found that overexpression of this form of RHAMM confers a partially transformed phenotype *in vitro*. In particular, these RHAMM overexpressers resembled transformed cells in their stellate morphology, and obvious nuclear overlapping, indicating loss of contact inhibition, overgrowth at confluence and focus formation (Alberts *et al.*, 1989). The morphological alterations implicates a portion of RHAMM as being a critical regulator of density dependant contact inhibition, a phenomenon relevant to cell growth and motile behavior (Abercrombie *et al.*, 1971; Bray, 1992). The cells' slightly reduced focal contacts, and recent evidence linking RHAMM to focal adhesion turnover (Hall *et al.*, 1994), implicates these contact sites as likely targets in RHAMM's effect.

Other ECM components and their receptors have been previously linked to tumorigenesis and malignancy. They include, thrombospondin (Castle *et al.*, 1993), tenascin (Borsi *et al.*, 1992), the urokinase receptor (Kariko *et al.*, 1993), and the integrins (Giancotti and Ruoslahti, 1990). Several lines of evidence have implicated the extracellular matrix component, HA, in transformation and metastasis (Knudson *et al.*, 1989; Turley, 1992; Fraser and Laurent, 1993). The HA receptor, CD44, has been linked to tumor growth (Sy *et al.*,

1991; Bartolazzi *et al.*, 1994) and metastasis (Günthert *et al.*, 1991; Herrlich *et al.*, 1993), and the RHAMM receptor has been found to be a critical regulator of tumor cell motility and invasion (Turley *et al.*, 1991; Hardwick *et al.*, 1992; Turley *et al.*, 1993; Wang *et al.*, submitted).

The RHAMM II (exons 6-14) overexpressing cells' (Clone 12) loss of contact inhibition and altered focal adhesions was consistent with other experiments, in which an alternate RHAMM IV4 cDNA (Entwistle *et al.*, submitted) and genomic DNA (Hall *et al.*, submitted), transfected into 10T½ cells, also affected contact inhibition but in these cells were completely transforming. Further complementing these results were studies in which the suppression of RHAMM expression in *ras*-transfected cells (C3) promoted a reversion from the transformed phenotype (Hall *et al.*, submitted). Therefore, since the transfection experiments yielded consistent results with respect to RHAMM overexpression being an important regulator of contact inhibition, only three clones that expressed variable levels of RHAMM were chosen for detailed analysis in this particular study.

Although the RHAMM overexpression experiments all resulted in the loss of cellular contact inhibition, a comparative analysis between the RHAMM II cDNA and both the RHAMM IV4 cDNA and genomic DNA transfections, revealed distinct differences in the extent with which cellular transformation was induced. The overexpression of the

proteins derived from the RHAMM IV4 cDNA (exons 1-14) and genomic DNA (exons 1-14), promoted complete cellular transformation, with the affected cells' exhibiting a malignant phenotype *in vitro* and *in vivo*. These overexpressing cells lost contact inhibition of growth, were highly motile, exhibited anchorage independent growth, formed fibrosarcomas when injected subcutaneously, and formed lung metastasis after intravenous injection. The cells also showed a definite loss in focal adhesions (Entwistle *et al.*, submitted; Hall *et al.*, submitted). Meanwhile, the overexpression of proteins derived from the RHAMM II cDNA (exons 6-14) (this study) was only partially transforming, in that the cells displayed a loss of contact inhibition of growth *in vitro*, and only slightly altered focal adhesions.

Focal adhesions have long been linked to cellular contact inhibition. These adhesive contacts are critical for maintaining the stable cell-substratum contacts most prevalent in non-transformed contact inhibited cells (Burridge *et al.*, 1988). With respect to cell motile behavior, stable focal contacts are present in sessile cells, and less stable ones occur in locomoting cells (Lo and Chen, 1994). These specialized junctions consist of a transmembrane integrin receptor which links extracellular matrix components, such as fibronectin, laminin, and collagen, to the cytoskeleton (Woods and Couchman, 1988). Their assembly involves a cascade of molecular interactions which include cytoplasmic,

transmembrane and extracellular components. According to the model (Alberts *et al.*, 1989), actin stress fibers are anchored to the plasma membrane via a complex of cytoplasmic plaque proteins that include talin, vinculin, α-actinin, and paxillin (Burridge *et al.*, 1988; Woods and Couchman, 1988; Lo and Chen, 1994). Other focal adhesion components localized to the cytoplasmic domain include protein kinase C (PKC) (Jaken *et al.*, 1989), src (Rohrschneider, 1980), focal adhesion kinase (FAK) (Schaller *et al.*, 1992) and proteases (Chen *et al.*, 1984; Beckerle *et al.*, 1987). The integrin family of receptors transmit information from the ECM to the inside of the cell via the G proteins, *src* and *rho*, and culminate in the cytoskeletal organizations relevant to cell growth (Giancotti and Mainiero, 1994) and locomotion (McCarthy and Turley, 1993). Evidence indicates that the signalling molecules, rho (Ridley and Hall, 1992; Ridley and Hall, 1992) and PKC (Woods and Couchman, 1992) are important regulatory molecules in focal adhesion assembly.

Evidence indicates that the expression and function of the integrins, the transmembrane domain of these contact sites, has been linked to the normalization of growth properties, cell-substratum stability, as well as the suppression of invasiveness. Its signalling and cytoskeletal elements have been reported to be critical to these effects (Juliano and Haskill, 1993; Giancotti and Mainiero, 1994; Juliano, 1994). In particular, the overexpression of the $\alpha_5\beta_1$

fibronectin integrin receptor promoted anchorage dependant growth in transformed chinese hamster ovary (CHO) cells and reduced its migratory behavior (Giancotti and Ruoslahti, 1990). Integrin expression has also been associated with the full organization of an extracellular matrix, and it is presumed that adhesion induced signals are associated with its promotion of contact inhibition (Giancotti and Ruoslahti, 1990). The overexpression of the cytoskeletal molecules, vinculin (Rodríguez Fernández *et al.*, 1992a; Rodríguez Fernández *et al.*, 1992b) and α-actinin (Glück *et al.*, 1993), which depend on integrins for proper assembly, are also responsible for partially reverting the transformed phenotype. Therefore, the alterations in the focal adhesions of RHAMM overexpressing cells, predicts that RHAMM counteracts the stabilizing action of integrins.

Consistent with RHAMM's effects on focal adhesions, a number of observations have linked focal adhesions to cellular transformation. While tumor cells often display reduced focal adhesions, the overexpression of the fibronectin $\alpha_5\beta_1$ integrin receptor temporally reverses the transformed phenotype (Giancotti and Ruoslahti, 1990; Varner *et al.*, 1992) and promotes focal adhesion assembly (Burridge *et al.*, 1988). Similarly, the overexpression of tensin, a focal adhesion protein involved in the assembly process, reverses transformation of NIH 3T3 cells (Lo and Chen, 1994). Meanwhile, thrombospondin, an ECM component, that has been

associated with focal adhesion disassembly (Murphy-Ullrich and Hook, 1989), promotes serum and anchorage independent growth of immortalized cell lines (Castle *et al.*, 1993). Another ECM protein, tenascin, is believed to enhance tumorigenesis (Borsi *et al.*, 1992) through its involvement in focal adhesion disassembly (Murphy-Ullrich *et al.*, 1991). Furthermore, antisense suppression of the focal adhesion protein, vinculin, promotes cellular transformation (Rodríguez Fernández *et al.*, 1993), while the overexpression of the protein promotes partial reversion of the transformed phenotype (Rodríguez Fernández *et al.*, 1992a; Rodríguez Fernández *et al.*, 1992b). Also, the specific targetting of truncated *v-src* to focal adhesions, rather than the nucleus or cytoplasm, induces transformation (Leibl and Martin, 1992). Together, the evidence emphasizes the importance of these structures in cellular transformation.

The finding in this study that elevated levels of the RHAMM II (exons 6-14) protein results in partially transforming effects that are linked to disruptions in the focal adhesions, is particularly consistent with the ECM molecules, tenascin (Borsi *et al.*, 1992) and thrombospondin (Castle *et al.*, 1993), effect on transformation. These molecules' effects on this property have also been reported to coincide with alterations in the structure of the focal contacts.

A variety of molecular alterations have been observed in

the focal contacts of transformed cells. These sites have been associated with increased tyrosine kinase activity and protease secretion, stress fiber disassembly, impaired extracellular matrix components, decreased integrin expression, as well as the diffuse distribution of the receptor at the cell surface (Burridge *et al.*, 1988; Ruoslahti and Giancotti, 1989; Hynes, 1990; Humphries *et al.*, 1993). Therefore, in light of the RHAMM overexpressing cells' morphological resemblance to transformed cells, it is likely that their reduced cell-substratum adhesiveness must also reflect similar molecular alterations.

Evidence indicates that RHAMM localizes to the cytosol, nucleus, extracellular medium and cell surface (Hardwick *et al.*, 1992; manuscript in preparation). Its cytosolic and nuclear presence has been determined by subcellular fractionation (unpublished data). The secreted and shed form of the protein has been detected by pulse chase and surface labelling studies (manuscript in preparation). RHAMM's cell surface existence has been confirmed by subcellular fractionation, FACS, surface iodination, and sensitivity of RHAMM staining to light protease treatment (Hardwick *et al.*, 1992; Klewes *et al.*, 1993). The RHAMM II (exons 6-14) overexpressing cells failed to show elevated levels of the soluble protein. However, although epitope tagging would have more clearly distinguished the transfected proteins from the endogenous ones, the presence of RHAMM in the nucleus, cytosol

and at the cell surface, suggests that these variants of RHAMM contributed to the phenotypic changes evident in the RHAMM overexpressing cells. Although the role of the RHAMM proteins at the various locations is presently unclear, cell surface RHAMM has been previously linked to cell locomotion and morphological transformation (Turley *et al.*, 1991; Hardwick *et al.*, 1992). These earlier studies have even shown that the RHAMM's surface expression, along with its ligand, HA, is associated with a loss of contact inhibition in chick heart fibroblasts (Turley *et al.*, 1985). As well, the ability of exogenously applied anti-RHAMM antibody to block locomotion suggests that cell surface associated RHAMM regulates this function (Turley *et al.*, 1991). RHAMM's intracellular signalling events are reported to occur in focal adhesions. The molecular mechanisms underlying cell surface RHAMM's effects implicate a protein tyrosine kinase signal transduction pathway that targets focal adhesion turnover (Hall *et al.*, 1994). It is possible that RHAMM, like CD44 (Noble *et al.*, 1993), may also regulate expression of critical genes.

In light of the evidence linking cell surface RHAMM to cytoskeletal reorganization, the motile phenotype, cellular transformation, and focal adhesions, it is predicted that the expression levels of functional surface RHAMM is critical to whether RHAMM induces a complete or partial transformation. Thus a possible model (Figure 16) depicting how genomic RHAMM

and RHAMM IV4 (exons 1-14) differed from RHAMM II (exons 6-14) in the extent with which cellular transformation was invoked, is speculated to be related to its efficient anchorage at the cell surface to mediate the appropriate signalling events. The additional 3' peptide sequence encoded in the RHAMM IV4 cDNA and genomic DNA, may be critical for efficient anchorage.

The RHAMM cDNAs and genomic DNA lack an obvious signal sequence or a hydrophobic domain long enough to span the membrane (Hardwick *et al.*, 1992; Entwistle *et al.*, submitted). Therefore, based on RHAMM's initial isolation as part of a complex of soluble proteins, RHAMM's cell surface localization was hypothesized to associate at the cell surface as the Hyaluronan Receptor Complex called HARC (Turley, 1989a). Its cell surface presence was predicted to require carrier proteins and/or an integral docking protein (Hardwick *et al.*, 1992; Entwistle *et al.*, submitted), like certain animal lectins (Barondes, 1988), the transferrin receptor (McClelland *et al.*, 1984), and the high affinity elastin/laminin receptors (Yow *et al.*, 1988; Rao *et al.*, 1989). In accordance with this, the additional peptide sequence encoded in the RHAMM IV4 cDNA and genomic DNA, may be critical for RHAMM to efficiently complex with the docking protein at the cell surface, as well as to associate with carrier proteins potentially required for its translocation to the surface. The overexpression and activation of this receptor protein is expected to elicit the signal transduction events critical to RHAMM's induction of

motile behavior and focal adhesion turnover. Since the overexpression of the RHAMM receptor is predicted to amplify the signals favoring focal adhesion disassembly (Hall *et al.*, 1994), its effects would counteract the stabilizing actions of integrins. The cytoskeletal reorganizations and decreased adhesiveness associated with the increased turnover, would help explain the transfected cells' loss of growth inhibition, increased motile rates, and the acquisition of tumorigenic capabilities *in vivo*. In this light, the partially transforming effects associated with the overexpression of the RHAMM II protein, may be contingent upon its lack of the peptide sequence (exon 4) critical for efficient anchorage to the docking protein. This would prevent the induction of the signalling events relevant to the cytoskeletal organizations associated with the motile phenotype, and thereby explain the incomplete cellular transformation.

The increased expression of RHAMM II at the cell surface, in spite of it lacking the critical exon 4 peptide sequence, may be due to its repeat sequences (21 amino acids repeated 5 times) mediating interactions with inappropriate carrier proteins. However, even though some of this truncated protein may be translocated to the surface, its functional capabilities would be limited by its lack of this critical peptide. In this context, it is possible that the cells' slight reduction in cell-substratum adhesions is partly due to signals generated when RHAMM's repeat sequences allow some

interaction with the hypothetical integral docking protein. However, since the interaction is inefficient it fails to induce the signal transduction events associated with complete cellular transformation.

Alternatively, an intracrine effect may well be predominantly responsible for these cells' loss of contact inhibition. This proposal is based on the fact that the cells' RHAMM surface expression was only slightly elevated above that of controls, and therefore the bulk of the protein must occur intracellularly. In this context, the slightly reduced focal adhesions may be attributed to a displacement effect, in which excess cytosolic RHAMM obstructs the protein interactions critical for stable focal adhesion assembly. RHAMM's repeat sequence may further complicate this effect by mediating protein associations which are detrimental to focal adhesion stability. The notion that excess RHAMM may interfere with protein recruitment from the diffusible pools throughout the cells and its subsequent targetting to the sites of assembly, is consistent with reports that inhibiting the mobilization of the cytoplasmic plaque protein, talin, corresponded with a reduction in cell focal contacts (Luna and Hitt, 1992). Therefore, it is conceivable that excess RHAMM impedes the mobilization of a number of focal adhesion constituents, including paxillin (Turner *et al.*, 1990), protein kinase C (PKC) (Jaken *et al.*, 1989), tyrosine kinases (Burridge *et al.*, 1988), *src* (Rohrshneider, 1980), FAK

(Schaller *et al.*, 1992), FAK related nonkinase (FRNK) (Schaller *et al.*, 1993), signal proteins containing SH2 and SH3 domains (Davis *et al.*, 1991), and the calcium dependant proteases (Beckerle *et al.*, 1987). Most notably, since Rho (Ridley and Hall, 1992), FAK (Burridge *et al.*, 1992), and PKC (Woods and Couchman, 1992), have been shown to be important in promoting focal adhesion assembly and actin organization, it is possible that RHAMM's phenotypic effects involve interfering with these proteins, and/or the factors regulating their activity (Bokoch and Der, 1993; Khosravi-Far and Der, 1994). Disrupting interactions between junctional molecules and the integrin receptor's cytoplasmic tail, may prevent the receptor clustering which is characteristic of stable focal adhesions (Humphries *et al.*, 1993). Additionally, if the focal contacts of the RHAMM overexpressing cells contain elevated levels of phosphorylated proteins, excess RHAMM may further complicate this effect and disrupt the normal signal transduction pathways associated with the cytoskeleton, by displacing the relevant substrates. Consistent with this, inappropriate phosphorylations of actin-binding proteins contribute to an altered morphology by hindering stress fiber organization (Lo and Chen, 1994).

In addition to a possible intracrine effect of RHAMM on focal adhesions being related to the displacement of cytoplasmic plaque proteins, it is possible that this effect also targets proteins associated with actin organization.

Although, the clones' actin organization was not examined, the cells' altered focal adhesions, stellate morphology, and the fact that 10T½ cells displayed highly organized stress fibers when RHAMM expression was diminished by antisense (unpublished data), predicts stress fiber disorganization to be relevant (Burridge *et al.*, 1988). Support for RHAMM's association with actin organization include: RHAMM's colocalization with actin (Turley *et al.*, 1990); immunodetection of RHAMM in a fibrillar pattern in control 10T½ fibroblasts (this study); and the similarity between the RHAMM HA binding domain's 1:9 motif and the actin binding motif (Aderem, 1992; Yang *et al.*, 1993). The 1:9 motif defines the amino acids critical for RHAMM's binding to HA. The domain specifically refers to a motif of B(X7)B, in which B represents any basic amino acid except histidine, and X represents any amino acid except an acidic one (Yang *et al.*, 1993). Therefore, if the RHAMM HA binding domain does indeed mediate interactions with actin, it is conceivable that at elevated levels, cytosolic RHAMM displaces actin binding proteins pivotal for stress fiber assembly and cytoskeletal organization (Pavalko and Burridge, 1991). Consistent with this proposal, transfection studies implicate this domain as being critical to conferring an altered cell morphology; 10T½ cells transfected with a RHAMM cDNA containing mutated HA binding domains, allowed 10T½ cells to retain normal contact inhibited behavior (personal communication), and permitted *ras*-transfected (C3) cells

transfected with mutated RHAMM reverted back to the contact inhibited state (Hall *et al.*, submitted).

Interestingly enough, the HA binding domain appears to be present in a number of other proteins, including polymerases (DNA-directed RNA polymerase), myosin, thrombospondin, and phospholipase C (personal communication). Therefore, it is plausible that this motif mediates important intracellular interactions, which may or may not include HA. In this respect, the elevated levels of the RHAMM protein may promote binding to these targets, and thereby prevent the relevant associations. Since such an effect has the potential to disrupt a number of important protein interactions, this may ultimately contribute to the altered cellular morphology and reduced cytoskeletal stability evident in the RHAMM overexpressing cells. Although these effects are speculative, and the four fold increase in RHAMM may not be physiologically relevant to cells, the evidence implicating the 1:9 motif as a key component in the morphological regulation of cells, and the presence of this sequence in other proteins, may be indicative of this domain's capacity to mediate intracellular interactions which may be potentially detrimental to the cell.

Evidence that the RHAMM II (exons 6-14) isoform occurred endogenously in fibroblasts and does not necessarily represent an incomplete cDNA of RHAMM I, includes the fact that the predicted protein size (52 kDa protein) matched the protein detected in the cell lysates of *ras*-transformed cells

(Hardwick *et al.*, 1992). The detection of a higher molecular weight protein in normal 10T½ cells, may reflect such posttranslational modifications as glycosylation and phosphorylation events (Hardwick *et al.*, 1992). Moreover, further support for the existence of a truncated RHAMM II cDNA includes the fact that several transcription start points (tsps) have been located within intron 5, upstream of the start codon (exon 6) for RHAMM II. Although epitope tagging studies, and the use of enzymes are needed to confirm these possibilities, these studies predict that part of RHAMM II's normal cellular function is related to its potential role as an intracellular HA binding protein, as well as at the cell surface.

FIGURE 16. A hypothetical model depicting a complete and partial function of surface RHAMM. RHAMM efficiently associates with the transmembrane docking protein when it contains the repeat sequence (21 amino acids repeated 5 times) and exon 4 (3' peptide sequence). The association results in an appropriate conformational change in the docking protein, and the transduction of signalling events favoring focal adhesion turnover. RHAMM inefficiently binds to the docking protein when it only contains the repeat sequence. Since *src* associates poorly with the docker, this results in little activation of the relevant signalling events.

CELL SURFACE RHAMM

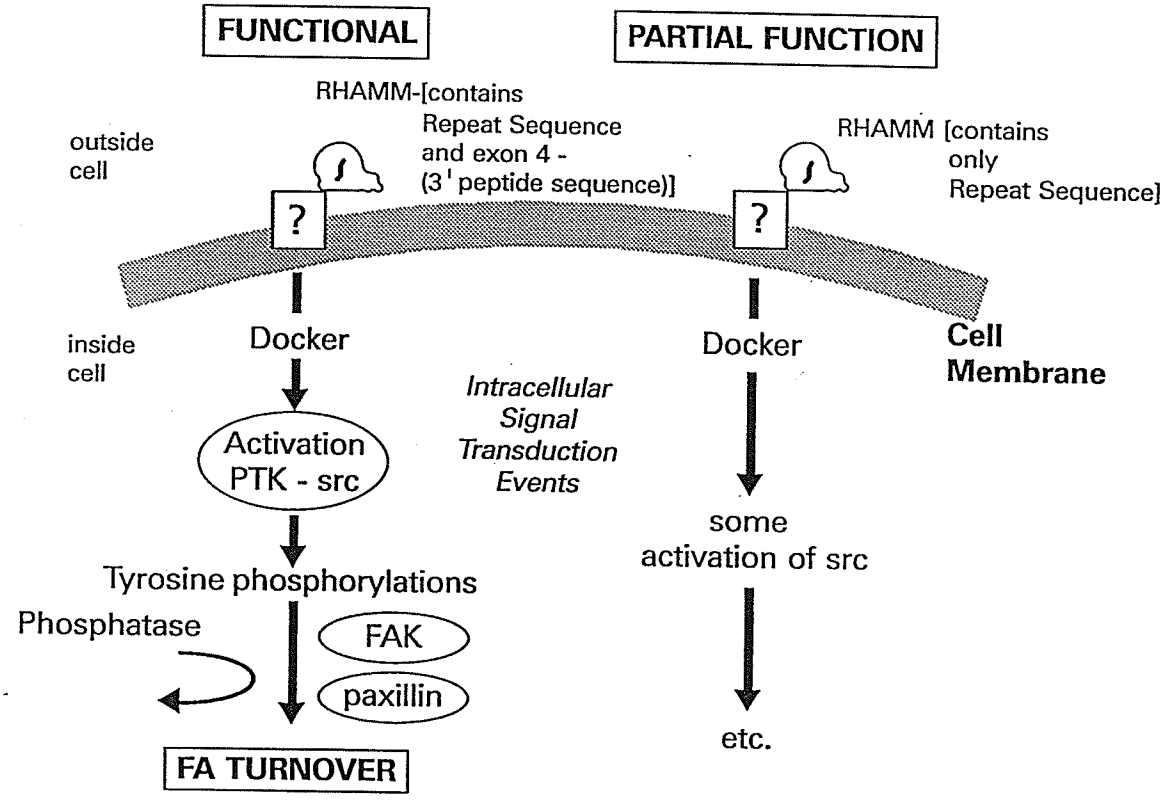

CONCLUSIONS

In conclusion, RHAMM overexpression appears to regulate cell contact behavior by altering focal adhesions. The proposed model suggests that although both surface and cytosolic RHAMM may modulate cell substratum adhesions, the expression of functional cell surface RHAMM, determines the extent of transformation. Both RHAMM forms are predicted to exert their anti-adhesive effects by destabilizing focal adhesions. Cytosolic RHAMM is speculated to promote a loss of contact behavior by disrupting the molecular interactions associated with integrin function and focal adhesion assembly. Surface RHAMM effects on transformation are believed to be more potent since it counteracts integrin function by enhancing signals which may affect events other than focal adhesion assembly. In particular, since integrin expression has been linked to metastasis and invasion *in vivo*, RHAMM overexpression may indirectly promote integrin expression associated with tumorigenesis, most notably those receptors involved in homing and cell survival. Future investigations which utilize the principles of epitope tagging, may more clearly distinguish transfected RHAMM from the endogenous one, and thereby allow for more ease in assessing the particular proteins' effects on cell behavior. At present, it is unclear if the cytoskeletal disruptions or RHAMM's regulation of focal adhesion turnover are sufficient to permit transformation, or whether RHAMM plays an instructive

(signalling) role in initiating cellular events, other than focal adhesions, which are critical for ultimately inducing the transformed phenotype. Clearly, however, this study further illustrates that a disruption in focal adhesions predisposes cells to transformation.

The overexpression of the RHAMM II isoform failed to promote malignant potential *in vivo* but was able to partially transform cells by promoting a loss of contact behavior. In light of the evidence that depicts RHAMM IV4 and genomic RHAMM overexpression as being associated with the induction of the malignant phenotype *in vivo* and *in vitro*, it appears that elevated levels of particular RHAMM forms, specifically the surface form, is critical to whether RHAMM induces either a partial or complete cellular transformation.

REFERENCES CITED

Abercrombie, M. 1970. Contact inhibition in tissue culture. *In vitro*. **6**:129-170.

Abercrombie, M., J.E.M. Heaysman, and S.M. Pegrum. 1970. The locomotion of fibroblasts in culture. I. Movements of the leading edge. *Exp. Cell. Res.* **59**:393-398.

Abercrombie, M., J. Heaysman, and S.M. Pegrum. 1971. The locomotion of fibroblasts in culture. *Exp. Cell. Res.* **67**:359-367.

Aderem, A. 1992. Signal transduction and the actin cytoskeleton: the roles of MARCKS and profilin. *TIBS*. **17**:438-443.

Albelda, S.M. 1993. Role of integrins and other cell adhesion molecules in tumor progression and metastasis. *Lab. Invest.* **68**:4-17.

Alberts, B., D. Bray, J. Lewis, M. Raff, K. Roberts, and J.D. Watson. 1989. Molecular Biology of the Cell. 2nd ed. Garland Publishing, Inc. New York and London. p.650-674.

Aznavoorian, S., A.N. Murphy, W.G. Stetler-Stevenson, and L.A. Liotta. 1993. Molecular aspects of tumor cell invasion and metastasis. *Cancer*. **71**:1368-1383.

Barondes, S.H. 1988. Bifunctional properties of lectins: lectins redefined. *Trends Biochem. Sci.* **13**:480-482.

Bartolazzi, A., R. Peach, A. Aruffo. and I. Stamenkovic. 1994. Interaction between CD44 and hyaluronate is directly implicated in the regulation of tumor development. *J. Exp. Med.* **180**:53-66.

Beckerle, M.C., K. Burridge, G.N. Demartino, and D.E. Croall. 1987. Colocalization of calcium dependent protease II and one of its substrates at sites of cell adhesion. *Cell*. **51**:569-577.

Behrens, J. 1993. The role of cell adhesion molecules in cancer invasion and metastasis. *Breast Canc. Res. Treat.* **24**:175-184.

Bokoch, G.M., and C.J. Der. 1993. Emerging concepts in the *Ras* superfamily of GTP-binding proteins. *FASEB*. **7**:750-759.

Borsi, L., B. Carnemolla, G. Nicolo, B. Spina, G. Tanara, and L. Zardi. 1992. Expression of different tenascin isoforms in normal hyperplastic and neoplastic human breast tissues. *Int. J. Canc.* **52**:688-692.

Boukerche, H., O. Berthier-Vergnes, M. Bailly, J.F. Dore, L.L.K. Leung, and J.L. McGregor. 1989. A monoclonal antibody (LyP18) directed against the blood platelet glycoprotein IIb/IIIa complex inhibits human melanoma growth *in vivo*. *Blood*. **74**:909-912.

Bray, D. 1992. Cell Movements. Garland Publishing, Inc. New York and London. p.17-59.

Burridge, K., K. Fath, T. Kelly, G. Nuckolls, and C. Turner. 1988. Focal adhesions: transmembrane junctions between the extracellular matrix and the cytoskeleton. *Annu. Rev. Cell Biol*. **4**:487-525.

Burridge, K., C.E. Turner, and L.H. Romer. 1992. Tyrosine phosphorylation of $pp125^{FAK}$ accompanies cell adhesion to the extracellular matrix: a role in cytoskeletal assembly. *J. Cell Biol*. **119**:893-903.

Butler, M. 1991. The characteristics and growth of cultured cells. *In* Mammalian Cell Biotechnology: A Practical Approach. Edited by M. Butler. Oxford University Press. p.1-24.

Castle, V.P., X. Ou, K. O'Rourke, and V.M. Dixit. 1993. High level thrombospondin expression in two NIH 3T3 cloned lines confers serum and anchorage-independent growth. *J. Biol. Chem*. **268**:2899-2903.

Chen, W.T., K. Olden, B.A. Bernard, and F. Chu. 1984. Expression of transformation-associated protease(s) that degrade fibronectin at cell contact site. *J. Cell. Biol*. **98**:1546-1555.

Damen, J.E., A.Y. Tagger, A.H. Greenberg, and J.A. Wright. 1989. Generation of metastatic variants in population of mutator and amplificator mutants. *J. Natl. Canc. Inst*. **81**:628-631.

Damsky, C. and Z. Webb. 1992. Signal transduction by integin receptors for extracellular matrix cooperative processing of extracellular information. *Curr. Opin. Cell. Biol*. **4**:772-781.

Davis, S., M.L. Lu, S.H. Lo, S. Lin, J.A. Butler, B.J. Druker, T.M. Roberts, Q. An, and L.B. Chen. 1991. Presence of an SH2 domain in the actin-binding protein tensin. *Science*. **252**:712-715.

Egan, S.E., G.A. McClarty, L. Jarolim, J.A. Wright, I. Spiro, G. Hager, and A.H. Greenberg. 1987. Expression of H-*ras* correlates with metastatic potential: evidence for direct regulation of the metastatic phenotype in $10T\frac{1}{2}$ and NIH 3T3 cells. *Mol. Cell. Biol*. **7**:830-837.

Entwistle, J., S. Zhang, B. Yang, C. Wong, C.L. Hall, G. Curpen, M. Mowat, A.H. Greenberg, and E.A. Turley. 1995. The molecular characterization of the gene encoding the hyaluronan receptor RHAMM. *Submitted*.

Felgner, P.L., T.R. Gadek, M. Holm, R. Roman, H.W. Chan, M. Wenz, J.P. Northrop, G.M. Ringold, and M. Danielsen. 1987. Lipofection: A highly efficient, lipid-mediated DNA-transfection procedure. *Proc. Natl. Acad. Sci. USA*. **84**:7413-7417.

Fraser, R. and T. Laurent. 1993. Hyaluronate. *FASEB*. **6**:2397-2404.

Giancotti, F.G. and E. Ruoslahti. 1990. Elevated levels of the $\alpha_5\beta_1$ fibronectin receptor suppress the transformed phenotype of chinese hamster ovary cells. *Cell*. **60**:849-859.

Giancotti, F.G., and F. Mainiero. 1994. Integrin-mediated adhesion and signalling in tumorigenesis. *Biochim. Biophy. Acta*. **1198**:47-64.

Gingras, M.C., L. Jarolim, J. Finch, G.T. Bowden, J.A. Wright, and A.H. Greenberg. 1990. Transient alterations in the expression of protease and extracellular matrix genes during metastatic lung colonization by H-*ras* transformed 10T½ fibroblasts. *Cancer Res*. **50**:4061-4066.

Glück, U., D.J. Kwiatkowski, and A. Ben-Ze'ev. 1993. Suppression of tumorigenicity in simian virus 40-transformed 3T3 cells transfected with α-actinin cDNA. *Proc. Natl. Acad. Sci. USA*. **90**:383-387.

Gunning, P., J. Leavitt, G. Muscat, S. Ng, and L. Kedes. 1987. A human B-actin expression vector system directs high-level accumulation of antisense transcripts. *Proc. Natl. Acad. Sci. USA*. **84**:4831-4835.

Günthert, U., M. Hofmann, W. Rudy, S. Reber, M. Zoller, I. Haubmann, S., Martzku, A. Wenzel, H. Ponta, and P. Herrlich. 1991. A new variant of glycoprotein CD44 confers metastatic potential to rat carcinoma cells. *Cell*. **65**:13-24.

Günthert, U. 1993. CD44: a multitude of isoforms with diverse functions. *Curr. Topics Microbio. Immunol*. **184**:47-63.

Hall, C.L., C. Wang, L.A. Lange, and E.A. Turley. 1994. Hyaluronan and the hyaluronan receptor RHAMM promote focal adhesion turnover and transient tyrosine kinase activity. *J. Cell Biol*. **126**:575-588.

Hall, C.L., L.A. Lange, D.A. Prober, and E.A. Turley. 1994. Hyaluronan:RHAMM promoted cell locomotion requires the tyrosine kinase protooncogene product $pp60^{c\text{-}src}$. (Abstract) *American Society for Cell Biology*.

Hall, C.L., B. Yang, X. Yang, S. Zhang, M. Turley, S. Shanti, L. Lange, C. Wang, G. Curpen, R.C. Savani, A.H. Greenberg, and E.A. Turley. 1995. Overexpression of the hyaluronan receptor RHAMM is transforming and is also required for H-*ras* transformation. *Submitted*.

Hardwick, C., K. Hoare, R. Owens, H.P. Hohn, M. Hook, D. Moore, V. Cripps, L. Austen, D.M. Nance, and E.A. Turley. 1992. Molecular cloning of a novel hyaluronan receptor that mediates tumor cell motility. *J. Cell. Biol.* **117:**1343-1350.

Harlow, E. and D. Lane. 1988. Antibodies. A laboratory manual. Cold Spring Harbor Laboratory Press, Cold Spring Harbor, New York. p.300.

Hart, I.R., M. Birch, J.F Marshall. 1991. Cell adhesion receptor expression during melanoma progression and metastasis. *Cancer and Metastasis Rev.* **10:**115-128.

Hynes, R.O. 1992. Integrins:versatility, modulation and signalling in cell adhesion. *Cell* **69:**11-25.

Herrlich, P., M. Zoller, S.T. Pals and H. Ponta. 1993. CD44 splice variants: metastases meet lymphocytes. *Immunology Today* **14:**395-399.

Humphries, M.J., A.P. Mould, and D.S. Tuckwell. 1993. Dynamic aspects of adhesion receptor function- integrins both twist and shout. *BioEssays*. **15:**391-397.

Iozzo, R.V. 1985. Proteogylcans: structure, function and role in neoplasia. *Lab. Invest.* **53:**373-396.

Jaken, S., K. Leach, and L.R. Klauk. 1989. Association of type 3 protein kinase C with focal contacts in rat embryo fibroblasts. *J. Cell. Biol.* **109:**687-704.

Jones, P.C., C. Schmidhauser, and M.J. Bissell. 1993. Regulation of gene expression and cell function by extracellular matrix. *Crit. Rev. Eukaryot. Gene. Expr.* **3:**137-154.

Juliano, R.L. and S. Haskill. 1993. Signal transduction from the extracellular matrix. *J. Cell. Biol.* **120:**577-585.

Juliano, R. 1994. Signal transduction by integrins and its role in the regulation of tumor growth. *Cancer and Metastasis Reviews* **13**:25-30.

Kariko, K., A. Kuo, D. Boyd, S.S. Okada, B.C. Clines, and E.S. Barnathan. 1993. Overexpression of urokinase receptor increases invasion without altering cell migration in human osteosarcoma cell line. *Cancer Res.* **53**:3109-3117.

Khosravi-Far, R., and C.J. Der. 1994. The *ras* signal transduction pathway. *Cancer and Metastasis Reviews*. **13**:67-89.

Kingston, R.E., P. Chomczynski, and N. Sacchi. 1993. Guanidinium method for total RNA preparation. *Cur. Prop. Mol. Biol,* (eds. Ausbel, F.M., Brent, R., Kingston, R., Moore, D.D., Seidman, J.G., Smith, J.A. and Struhl, K.) John Wiley and Sons, N.Y. p.421-428.

Klewes, L., E.A. Turley, and P. Prehm. 1993. The hyaluronate synthase from a eukaryotic cell line. *Biochem. J.* **290**:791-795.

Knudson, W., C. Biswas, and B.P. Toole. 1984. Interactions between human tumor cells and fibroblasts stimulate hyaluronate synthesis. *Proc. Natl. Acad. Sci. USA.* **81**:6767-6771.

Knudson, W., C. Biswas, X.Q. Li, R.E. Nemec, and B.P. Toole. 1989. The role and regulation of tumor-associated hyaluronan. *In* The biology of hyaluronan. *Ciba Found. Symp.* **143**:150-169.

Knudson, C.B., and W. Knudson. 1990. Similar epithelial-stroma interactions in the regulation of hyaluronate production during limb morphogenesis and tumor invasion. *Cancer Lett.* **52**:113-122.

Knudson, C.B. and W. Knudson. 1993. Hyaluronan binding proteins in development, tissue homeostasis and disease. *FASEB.* **7**:1233-1241.

Laemmli, U.K. 1970. Cleavage of structural proteins during the assembly of the head of bacteriophage T4. *Nature (Lond.)* **227**:680-685.

Leibl, E.C. and G.S. Martin. 1992. The intracellular targetting of $pp60^{src}$ expression: localization to adhesion plaques is sufficient to transform chicken embryo fibroblasts. *Oncogene*. **7**:2412-2428.

Liotta, A. 1992. Cancer cell invasion and metastasis. *Scientific American*. 54-63.

Lo, S.H., and L.B. Chen. 1994. Focal adhesion as a signal transduction organelle. *Cancer and Metastasis Reviews* **13:**9-24.

Luna, E.J., and A.L. Hitt. 1992. Cytoskeleton-plasma membrane interactions. *Science*. **258:**955-963.

McCarthy, J. and E.A. Turley. 1994. Effects of extracellular matrix components on cell locomotion. *Crit Rev in Oral Bio and Med*. **4:**619-637.

McClelland, A., L.C. Kuhn, and F.H. Ruddle. 1984. The human transferrin receptor gene: genomic organization and the complete primary structure of the receptor deduced from a cDNA sequence. *Cell*. **39:**267-274.

Murphy-Ullrich, J.E., and M. Hook. 1989. Thrombospondin modulates focal adhesions in endothelial cells. *J. Cell. Biol*. **109:**1309-1312.

Murphy-Ullrich, J.E., V.A. Lightner, I. Aukhil, Y.Z. Yan, H.P. Erickson, and M. Hook. 1991. Focal adhesion integrity is downregulated by the alternatively spliced domain of human tenascin. *J. Cell. Biol*. **115:**1127-1136.

Noble, P.W., F.R. Lake, P.M. Henson, and D.W.H. Riches. 1993. Hyaluronate activation of CD44 induces insulin-like growth factor expression by a tumor necrosis factor α dependent mechanism in murine macrophages. *J. Clin. Invest*. **91:**2368-2377.

Pavalko, F.M., and K. Burridge. 1991. Disruption of the actin cytoskeleton after microinjection of proteolytic fragments of α-actinin. *J. Cell. Biol*. **114:**481-491.

Plantefaber, L.C. and R.O. Hynes. 1989. Changes in integrin receptors on oncogenically transformed cells. *Cell*. **56:**281-290.

Porter, K.R., G.J. Todaro, and V. Fonte. 1973. A scanning electron microscope study of surface features of viral and spontaneous transformants of mouse BALB/3T3 cells. *J. Cell Biol*. **59:**633-642.

Qian, F., D.L. Vaux, and F.L. Weissman. Expression of the integrin $\alpha_4\beta_2$ on melanoma cells can inhibit the invasive stage of metastasis formation. *Cell*. **77:**335-347.

Rao, C.N., V. Castronova, M.C. Schmitt, U.M. Wewer, A.P. Claysmith, L.A. Liotta, and M.E. Sobel. 1989. Evidence for a precursor of the high affinity metastasis-associated murine laminin receptor. *Biochemistry*. **28:**7476-7486.

Ratner, S. 1992. Lymphocyte migration through extracellular matrix. *Invasion Met.* **12:**82-100.

Ridley, A.J. and A. Hall. 1992. The small GTP-binding protein rho regulates the assembly of focal adhesions and actin stress fibers in response to growth factors. *Cell.* **70:**389-399.

Ridley, A.J. and A. Hall. 1992. Distinct patterns of actin organization regulated by the small GTP-binding proteins Rac and Rho. *Cold Spring Harbor Symp Quant Bio.* **LVII:**661-671.

Rodríguez Fernández, J.L., B. Geiger, D. Salomon, I. Sabanay, M. Zöller, and A. Ben-Ze'ev. 1992a. Suppression of tumorigenicity in transformed cells after transfection with vinculin cDNA. *J. Cell Biol.* **119:** 427-438.

Rodríguez Fernández, J.L., B. Geiger, D. Salomon, and A. Ben-Ze'ev. 1992b. Overexpression of vinculin suppresses cell motility in Balb/C 3T3 cells. *Cell. Motil. Cytoskeleton.* **22:**127-134.

Rodríguez Fernández, J.L., B. Geiger, D. Salomon and A. Ben-Ze'ev. 1993. Suppression of vinculin expression by antisense transfection confers changes in cell morphology, motility, and anchorage-dependent growth of 3T3 cells. *J. Cell Biol.* **122:**1285-1294.

Rohrshneider, L.R. 1980. Adhesion plaques of Rous sarcoma virus-transformed cell contain the *src* gene product. *Proc. Natl. Acad. Sci. USA.* **77:**3514-1518.

Ruoslahti, E. and F.G. Giancotti. 1989. Integrins and tumor cell dissemination. *Cancer Cells.* **1:**119-126.

Ruoslahti, E. 1992. Control of cell motility and tumour invasion by extracellular matrix interactions. *Br. J. Cancer.* **66:**239-242.

Sage, E.H. and P. Bornstein. 1991. Extracellular proteins that modulate cell-matrix interactions. *J. Biol. Chem.* **266:**14831-14834.

Sambrook, J., F.F. Fritsch, and T. Maniatis. 1989. Molecular cloning: A laboratory manual. 2nd ed. Cold Spring Harbor Laboratory Press, Cold Spring Harbor, New York.

Samuel, S.K., R.A.R. Hurta, M.A. Spearman, J.A. Wright, E.A. Turley, and A.H. Greenberg. 1993. TGF-$ß_1$ stimulation of cell locomotion utilizes the hyaluronan receptor RHAMM and hyaluronan. *J. Cell Biol.* **123:**749-758.

Savani, R., C. Wang, B. Yang, M. Kinsella, R. Stern, T. Wight, and E.A. Turley. 1993. Molecular mechanisms of smooth muscle cell migration following wounding injury: the role of hyaluronan and RHAMM. *Submitted*.

Schaller, M.D. C.A. Borgman, B.S. Cobb, R.R. Vines, A.B. Reynolds, and J.T. Parsons. 1992. $pp125^{FAK}$, a structurally unique protein tyrosine kinase associated with focal adhesions. *Proc. Natl. Acad. Sci. USA*. **89:**5192-5196.

Schaller, M.D., C.A. Borgman, and J.T. Parsons. 1993. Autonomous expression of a noncatalytic domain of the focal adhesion-associated protein tyrosine kinase $pp125^{FAK}$. *Mol. Cell. Biol.* **13:**785-791.

Schreiner, C., M. Fisher, S. Mussein, and R.L. Juliano. 1991. Increased tumorigenicity of fibronectin receptor deficient Chinese hamster ovary cell variants. *Cancer Res.* **51:**1738-1740.

Schwartz, M.A. 1993. Signalling by integrins:implications for tumorigenesis. *Cancer Res.* **53:**1503-1506.

Stetler-Stevenson, W.G., S. Aznavoorian, and L.A. Liotta. 1993. Tumor cell interactions with the extracellular matrix during invasion and metastasis. *Amer. Rev. Cell. Biol.* **9:**541-573.

Sy, M.S., Y.J. Guo, and I. Stamenkovic. 1991. Distinct effects of two CD44 isoform on tumor growth in vivo. *J. Exp. Med.* **174:**859-866.

Symington, B.E. 1990. Fibronectin receptor overexpression and loss of transformed phenotype in a stable variant of the K562 cell line. *Cell Regul.* **1:**637-648.

Thomas, L., H. Randolph Byers, J. Vink, I. Stamenkovic. 1992. CD44H regulates tumor cell migration on hyaluronate-coated substrate. *J. Cell. Bio.* **118:**971-977.

Turley, E.A. 1984. Proteoglycans and cell adhesion: their putative role during tumorigenesis. *Cancer Metastasis Rev.* 3:325-339.

Turley, E.A., and M. Tretiak. 1985. Glycosaminoglycan production by murine melanoma variants *in vivo* and *in vitro*. *Cancer Res.* **45:**5098-5105.

Turley, E.A., P. Bowman, and M.A. Kytryk. 1985. Effects of hyaluronate and hyaluronate binding proteins on cell motile and contact behavior. *J. Cell Sci.* **78:**133-145.

Turley, E.A., D. Moore, and L.J. Hayden. 1987. Characterization of hyaluronate binding proteins isolated from 3T3 and murine sarcoma virus transformed 3T3 cells. *Biochem.* **26:**2997-3005.

Turley, E.A. 1989. The role of a cell-associated hyaluronan-binding protein in fibroblast behaviour. *In* Biology of Hyaluronan. *Ciba Found. Symp.* **143:**121-137.

Turley, E.A., P. Brassel, and D. Moore. 1990. A hyaluronan-binding protein shows a partial and temporally regulated codistribution with actin on locomoting chick heart fibroblasts. *Exp. Cell Res.* **187:**243-249.

Turley, E.A., L. Austen, K. Vandeligt, and C. Clary. 1991. Hyaluronan and a cell-associated hyaluronan binding protein regulate the locomotion of *ras*-transformed cells. *J. Cell Biol.* **112:**1041-1047.

Turley, E.A. 1992. Hyaluronan and cell locomotion. *Cancer Metastasis Rev.* **11:**21-30.

Turley, E.A., L. Austen, D. Moore, and K. Hoare. 1993. *Ras*-transformed cells express both CD44 and RHAMM hyaluronan receptors: Only RHAMM is essential for hyaluronan-promoted locomotion. *Exp. Cell. Res.* **207:**277-282.

Turley, E.A., A.J. Belch, S. Poppema, and L.M. Pilarski. 1993. Expression and function of a receptor for hyaluronan-mediated motility on normal and malignant B lymphocytes. *Blood.* **81:**446-453.

Turner, C.E., J.R. Glenney, and K. Burridge. 1990. Paxillin: A new vinculin-binding protein present in focal adhesions. *J. Cell Biol.* **111:**1059-1068.

Varner, J.A., M.H. Fisher, and R.L. Juliano. 1992. Ectopic expression of integrin $\alpha_5\beta_1$ suppresses *in vitro* growth and tumorigenicity of human colon carcinoma cells. *Mol. Biol. Cell.* **3:**232a

Wang, C., S. Zhang, R. Stern, and E.A. Turley. 1994. Hyaluronan receptor regulates human breast cancer motility and invasion *in vitro* and is overexpressed by breast carcinoma *in vivo. Submitted.*

Weston, J.A., and K.L. Hendricks. 1972. Reversible transformation by urea of contact-inhibited fibroblasts. *Proc. Natl. Acad. Sci. USA* **60:**3727-3731.

Woods, A. and J.R. Couchman. 1988. Focal adhesions and cell-matrix interactions. *Collagen Rel Res.* **8:**155-182.

Woods, A. and J.R. Couchman. 1992. Protein kinase C involvement in focal adhesion formation. *J. Cell Science*. **101:**277-290.

Yang, B., L. Zhang, and E.A. Turley. 1993. Identification of two hyaluronan-binding domains in the hyaluronan receptor RHAMM. *J. Biol. Chem.* **268:**8617-8623.

Yow, H., J.M. Wong, H.S. Chen, C. Lee, G.D. Steele, Jr. and L.B. Chen. 1988. Increased mRNA expression of a laminin-binding protein in human colon carcinoma: complete sequence of full length cDNA encoding the protein. *Proc. Natl. Acad. Sci. USA*. **85:**6394-6398.

Zetter, B. 1990. The cellular basis of site-specific tumor metastasis. *N. Engl. J. Med.* **322:**605-612.